

# Continuous variable quantum teleportation using non-Gaussian two mode squeezed coherent state

SHIKHAR ARORA

A thesis submitted for the partial fulfilment of  
BS-MS dual degree in Science



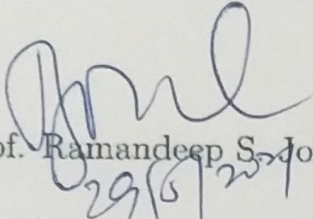
Department of Physical Sciences  
Indian Institute of Science Education & Research Mohali  
Knowledge city, Sector 81, SAS Nagar, Manauli PO, Mohali 140306, Punjab, India.

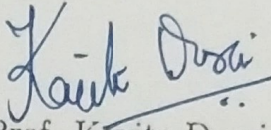
May 2021

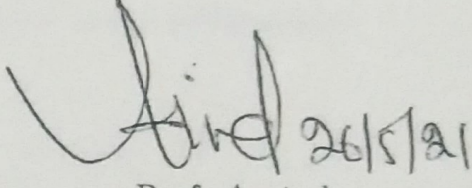


## Certificate of Examination

This is to certify that the dissertation titled "Continuous variable quantum teleportation using non-Gaussian two mode squeezed coherent state" submitted by Shikhar Arora (Reg. No. MS16055) for the partial fulfilment of BS-MS dual degree program of the Institute, has been examined by the thesis committee duly appointed by the Institute. The committee finds the work done by the candidate satisfactory and recommends that the report be accepted.

  
Prof. Ramandeep S. Johal  
29/5/21

  
Prof. Kavita Dorai

  
Prof. Arvind  
(Supervisor)  
26/5/21

Dated: May 26, 2021

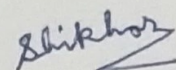




## Declaration

The work presented in this dissertation has been carried out by me under the guidance of Prof. Arvind at the Indian Institute of Science Education and Research (IISER) Mohali.

This work has not been submitted in part or in full for a degree, a diploma, or a fellowship to any other university or institute. Whenever contributions of others are involved, every effort is made to indicate this clearly, with due acknowledgement of collaborative research and discussions. This thesis is a bonafide record of original work done by me and all sources listed within have been detailed in the bibliography.

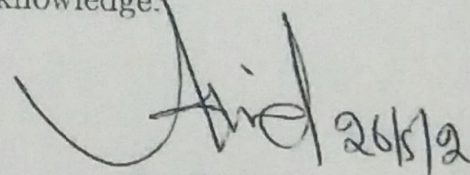


Shikhar Arora

(MS16055)

Dated: May 26, 2021

In my capacity as the supervisor of the candidate's project work, I certify that the above statements by the candidate are true to the best of my knowledge.



Prof. Arvind

(Supervisor)



*Dedicated to my twin  
(i owe my music to you)*





## Acknowledgements

Sometimes we are too close to a puzzle to see the bigger picture that is forming. I would like to thank my colleague and friend Dr. Chandan Kumar who closely saw the development of the research problem. While we were working minutely on the problem, Prof. Arvind's keen eye for the bigger picture helped steer us in the directions we would not otherwise explore. He is at the center of the development of this thesis and his expertise, kindness and vision cannot be appreciated enough. I wish to thank Prof. Kavita Dorai and Prof. Ramandeep Johal for agreeing to be a part of the committee that assesses this document. I am positively reinforced by Prof. Kavita's warm, welcoming tone and resonate with Prof. Johal's poetic inclination.

It is not easy to explain to my parents and some of my friends about the esoteric work that I do. Nevertheless they are curious and supportive and I am grateful to them for that. I gratefully acknowledge IISER Mohali for various facilities, especially the Library and DST for the INSPIRE funding that lives up to its name.

Finally I give here a list of quotes that inspired me. "You are an idiot, shikhi boi", "I had accepted that you'd never come" (that's what she said), "How is your wife and my kids?", "Balle Balle 100 rupye me shadi karle", "Kaali Beyi te milaange" (to the nights divine and ghostly), "Meetha hai tu" (Kadda hai tu), "Ek hi kaafi hai" and "Fourth of July" (Thank you Sufjan Stevens).

Shikhar.



# Abstract

Quantum Teleportation allows the transfer of an unknown quantum state between two distant physical systems. Here we consider the teleportation of a quantum state using various non-Gaussian entangled resource states, which are generated by a set of non-Gaussian operations on the two mode squeezed coherent (TMSC) state. To that end, we derive the Wigner characteristic function of the resource states, which is utilised in the derivation of the fidelity of teleportation. We show that coherence, defined as the amount of displacement of the vacuum state, yields better fidelity of teleportation in certain cases, when compared to non-Gaussian two mode squeezed vacuum (TMSV) state. Our analysis is very general and therefore, many previous results can be generated as a special case of our result.



# Contents

<b>1</b>	<b>Introduction</b>	<b>1</b>
1.1	Quantum Optical Systems . . . . .	3
1.1.1	Field Quantization . . . . .	3
1.1.2	Continuous Variable System . . . . .	9
1.2	Continuous Variable Teleportation . . . . .	13
1.2.1	Teleportation using TMSV state . . . . .	14
<b>2</b>	<b>Non-Gaussian Operations on TMSC state</b>	<b>17</b>
2.1	Non-Gaussian operations on one mode . . . . .	17
2.2	Non-Gaussian operations on both modes . . . . .	20
<b>3</b>	<b>Non-Gaussian Resource States in CV Teleportation</b>	<b>25</b>
3.1	Asymmetric Case . . . . .	25
3.1.1	Photon Subtraction on one mode of TMSC state . . . . .	25
3.1.2	Photon Addition on one mode of TMSC state . . . . .	27
3.1.3	Photon Catalysis on one mode of TMSC state . . . . .	28
3.2	Symmetric Case . . . . .	30
3.2.1	Photon Subtraction on both modes of TMSC state . . . . .	30
3.2.2	Photon Addition on both modes of TMSC state . . . . .	31
3.2.3	Photon Catalysis on both modes of TMSC state . . . . .	33
<b>4</b>	<b>Conclusion</b>	<b>35</b>
	<b>Bibliography</b>	<b>37</b>





# List of Figures

1.1	A single-mode radiation field in a one-dimensional cavity. . . . .	4
1.2	The energy levels in a quantum harmonic oscillator. . . . .	5
2.1	Schematic for non-Gaussian operation on one of the modes of two mode squeezed coherent (TMSC) state. . . . .	18
2.2	Schematic for non-Gaussian operation on both of the modes of two mode squeezed coherent (TMSC) state. . . . .	21
3.1	Fidelity (F) vs squeezing parameter (r) of teleportation for one-photon-subtracted two mode squeezed coherent (1-PSTMSC) state. . . . .	26
3.2	Fidelity (F) vs displacement (d) of teleportation for one-photon-subtracted two mode squeezed coherent (1-PSTMSC) state. . . . .	26
3.3	Fidelity (F) vs squeezing parameter (r) of teleportation for one-photon-added two mode squeezed coherent (1-PATMSC) state. . . . .	27
3.4	Fidelity (F) vs displacement (d) of teleportation for one-photon-added two mode squeezed coherent (1-PATMSC) state. . . . .	28
3.5	Fidelity (F) vs squeezing parameter (r) of teleportation for one-photon-catalysed two mode squeezed coherent (1-PCTMSC) state. . . . .	29
3.6	Fidelity (F) vs displacement (d) of teleportation for one-photon-catalysed two mode squeezed coherent (1-PCTMSC) state. . . . .	29
3.7	Fidelity (F) vs squeezing parameter (r) of teleportation for one-photon-subtracted (on both modes) two mode squeezed coherent (1,1)-PSTMSC state. . . . .	30
3.8	Fidelity (F) vs displacement (d) of teleportation for one-photon-subtracted (on both modes) two mode squeezed coherent (1,1)-PSTMSC state. . . . .	31

3.9	Fidelity (F) vs squeezing parameter (r) of teleportation for one-photon-added (on both modes) two mode squeezed coherent (1,1)-PATMSC state. . . . .	32
3.10	Fidelity (F) vs displacement (d) of teleportation for one-photon-added (on both modes) two mode squeezed coherent (1,1)-PATMSC state. .	32
3.11	Fidelity (F) vs squeezing parameter (r) of teleportation for one-photon-catalysed (on both modes) two mode squeezed coherent (1,1)-PCTMSC state. . . . .	33
3.12	Fidelity (F) vs displacement (d) of teleportation for one-photon-catalysed (on both modes) two mode squeezed coherent (1,1)-PCTMSC state. .	34

# Chapter 1

## Introduction

The notion of the physical state of a system is crucial in physics as well as in other disciplines. Any physical theory that aims to explain the development of a system needs to define the state of that system. For example, the state of a solid ball can be given by its position and momentum, and using Newtonian equations of motion, we can predict its position and momentum at a future time  $t$ . We can also include the angular momentum of the ball in the state, and use principles of rigid body dynamics to get a better description of the system with time.

We could consider a macroscopic system, like particles immersed in a viscous fluid or an air balloon. Such systems can be characterised by quantities like temperature, pressure, composition etc. This description, however, leaves out some information about the system, like the details of the microscopic constituents. Instead, if we consider a single particle or a lower number of particles, both classical and quantum mechanics assume that a proper physical state should include all possible information about the system. It is possible to consider and work with a common terminology of physical states for both classical and quantum systems. But, the difference in the underlying structure leads to significant points of departure between the two descriptions at both the mathematical and conceptual levels [12].

In classical mechanics, a system can be described using the Hamiltonian formalism. Here, the basic mathematical object is the phase space  $\Gamma$  of  $2n$  even dimensions. The physical observable or properties of the system are represented by a dynamical variable  $A(\mathbf{q}, \mathbf{p})$ , which is a real-valued function on  $\Gamma$ , where  $\mathbf{q}$  and  $\mathbf{p}$  are  $n$  generalised coordinates and their conjugate momenta respectively. A pure state is represented by a single point  $(\mathbf{q}_0, \mathbf{p}_0) \in \Gamma$ . Every  $A$  has a definite numerical value  $A(\mathbf{q}_0, \mathbf{p}_0)$  corresponding to this state - no spread or dispersion and no need or role for probabilities at

the level of pure states. These states are the cases of maximum possible information.

In quantum mechanics, on the other hand, the basic mathematical object is a Hilbert space  $H$ : a complex linear vector space with Hermitian non-negative inner product. The dimensions of this space  $H$  can be finite or infinite, depending on the quantum mechanical system. The physical observable or properties of the system are represented by Hermitian operators  $\hat{A}, \hat{B}$  etc. acting on  $H$ . A pure state is represented by a non-zero normalised vector  $|\psi\rangle$  in  $H$ . Although this is the state with maximum possible information, but even for such states probabilities of a quantum mechanical nature play an essential role. For example, consider a dynamical variable  $\hat{A}$  with discrete and real eigenvalues  $\{a_i\}$  corresponding to the orthonormal set of eigenkets  $\{|\phi_i\rangle\}$ . If we perform a measurement of  $\hat{A}$  using an appropriate experimental arrangement, the result comes out to be one of the eigenvalues  $\{a_i\}$  and the probability of getting that  $a_i$  is  $|\langle\phi_i|\psi\rangle|^2$ . These are irreducible quantum mechanical probabilities that are not caused by any inadequacy of knowledge about the system.

As we discussed that even in a state with maximum possible information, probabilities of quantum mechanical nature creep in the description of measurement. As if in compensation for this, and in fact leading to a great simplification, we have the principle of superposition of states, while dealing of course with pure states. Here is a quote from Dirac's discussion of this important principle in quantum mechanics: "... assume that between these states there exist peculiar relationships such that whenever the system is definitely in one state we can consider it as being partly in each of two or more other states ... the intermediate character of the state formed by superposition (thus) expresses itself through the probability of a particular result for an observation being intermediate between the corresponding probabilities for the original states, not through the result itself being intermediate between the corresponding results for the original states" [12, 11, 1].

Here we have discussed a rather simple distinction between quantum systems and classical systems. There are many interesting cases that come up in the composite systems or mixed states, which have been discussed in the references. Furthermore, many quantum foundation concepts discuss hidden variable theories that claim that there is more information in a system than perceived in its physical state [14, 20].

## 1.1 Quantum Optical Systems

The seeds of quantum mechanics go back to the minor issues of classical physics related to the nature of black body radiations and photoelectric effect. Planck, though an inherently conservative theorist, proposed that thermal radiations were absorbed and emitted in discrete quanta, to explain the spectra of thermal bodies. Einstein later generalised this idea, so that the quanta, rather than representing the absorption-emission process, represented light itself. He further described how matter and radiation can come into equilibrium, introducing the idea of stimulated emission, and how the photoelectric effect could be explained [18, 3].

In the early 1960s, the laser was invented and the subsequent development, like tune-able lasers in 1970s, led to an increase in the precision with which light could be produced and controlled. This enabled a systematic investigation of quantum properties of optical fields: quantum optics. The framework for the quantization of electromagnetic fields was given by Dirac in the early days of quantum mechanics. But the new technological possibilities led Glauber, Louisell etc. to lay the theoretical basis for the description of the laser. Signatures of non-classical light were soon identified, which accelerated the research in this field. Here, we introduce some basic theoretical ideas related to the quantum mechanical description of light and quantum states of light [18].

### 1.1.1 Field Quantization

Consider a single-mode radiation field confined in a one-dimensional cavity of length  $L$ , with perfectly conducting walls as shown in Fig. 1.1. The electric field vanishes on the boundaries and the mode is selected such that we get a standing wave. We assume a closed cavity and the field is assumed to be polarised in x-direction. The single mode field satisfying the Maxwell's equations and the boundary conditions is given by

$$\begin{aligned} E_x(z, t) &= \left( \frac{2\omega^2}{V\epsilon_0} \right)^{1/2} q(t) \sin(kz) \\ B_y(z, t) &= \left( \frac{\mu_0\epsilon_0}{k} \right) \left( \frac{2\omega^2}{V\epsilon_0} \right)^{1/2} \dot{q}(t) \cos(kz) \end{aligned} \tag{1.1}$$

where  $\omega$  is the frequency of the mode (mode selection for standing wave implies  $\omega = c(m\pi/L)$ , where  $m$  is a natural number) and  $k$  is the wave number, such that  $k = \omega/c$ ,  $V$  is the effective volume of the cavity and  $q(t)$  is a time-dependent factor having the dimension of length; this acts as the canonical position. Further,  $\dot{q}(t)$  (or  $p(t)$ , assuming mass variable to be unity) plays the role of a canonical momentum in these equations [7].

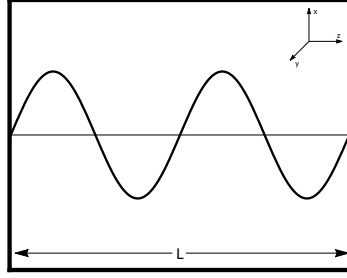


Figure 1.1: A single-mode radiation field in a one-dimensional cavity.

For this single-mode field, the classical field energy or Hamiltonian is given by

$$\begin{aligned}
 H &= \frac{1}{2} \int dV \left[ \epsilon_0 E_x^2(z, t) + \frac{1}{\mu_0} B_y^2(z, t) \right] \\
 &= \frac{A}{2} \int dz \left[ \epsilon_0 E_x^2(z, t) + \frac{1}{\mu_0} B_y^2(z, t) \right] \\
 &= \frac{A}{2} \int dz \left[ \left( \frac{2\omega^2}{V} \right) q^2 \sin^2 kz + \left( \frac{2\mu_0 \epsilon_0 \omega^2}{V k^2} \right) \dot{q}^2 \cos^2 kz \right] \quad (1.2) \\
 &= \frac{AL}{4} \left[ \left( \frac{2\omega^2}{V} \right) q^2 + \left( \frac{2\omega^2}{V k^2 c^2} \right) \dot{q}^2 \right] \\
 &= \frac{1}{2} (\omega^2 q^2 + p^2)
 \end{aligned}$$

It seems from the above simplification of Hamiltonian that a single-mode field is equivalent to a harmonic oscillator of unit mass. In this equivalence, the electric and magnetic field play the roles of canonical position and momentum, apart from some scalar factors.

### Quantum Harmonic Oscillator

Having identified the canonical variables  $q$  and  $p$  for the classical system, we use the correspondence rule and replace them with their operator equivalents in quantum



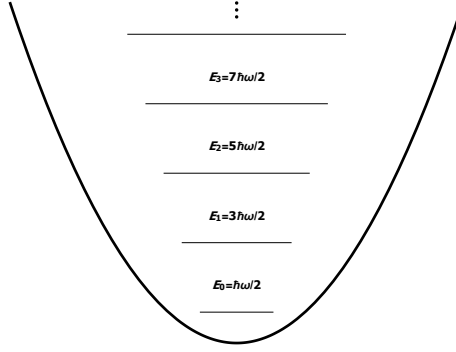


Figure 1.2: The energy levels in a quantum harmonic oscillator.

mechanics:  $\hat{q}$  and  $\hat{p}$ . These operators satisfy the canonical commutation relation  $[\hat{q}, \hat{p}] = i\hbar\mathbb{I}$ . The Hamiltonian finally becomes

$$\hat{H} = \frac{1}{2}(\omega^2 \hat{q}^2 + \hat{p}^2) \quad (1.3)$$

The operators  $\hat{q}$  and  $\hat{p}$  are self-adjoint (or Hermitian) and hence correspond to observable quantities. However, during the analytical treatment of quantum harmonic oscillator, it is convenient and traditional to introduce the annihilation ( $\hat{a}$ ) and creation ( $\hat{a}^\dagger$ ) operators, which are not self-adjoint and hence do not correspond to observable quantities.

$$\begin{aligned} \hat{H} &= \frac{1}{2}(\omega^2 \hat{q}^2 + \hat{p}^2) \\ &= \frac{\hbar\omega}{2} \left[ \left( \frac{\hat{q}}{q_0} - i \frac{\hat{p}}{p_0} \right) \left( \frac{\hat{q}}{q_0} + i \frac{\hat{p}}{p_0} \right) + 1 \right] \\ &= \hbar\omega \left[ \left( \frac{\hat{X}_1 - i\hat{X}_2}{\sqrt{2}} \right) \left( \frac{\hat{X}_1 + i\hat{X}_2}{\sqrt{2}} \right) + \frac{1}{2} \right] \\ &= \hbar\omega \left[ \hat{a}^\dagger \hat{a} + \frac{1}{2} \right] \end{aligned} \quad (1.4)$$

here  $q_0 = \sqrt{\hbar/2\omega}$  and  $p_0 = \sqrt{\hbar\omega/2}$ .  $\hat{X}_1$  and  $\hat{X}_2$  are dimensionless forms of the canonical variables, also known as quadrature operators. The non-Hermitian annihilation and creation operators follow simple commutation relations:  $[\hat{a}, \hat{a}^\dagger] = \hat{I}$ ,  $[\hat{a}, \hat{H}] = \hbar\omega \hat{a}$  and  $[\hat{a}^\dagger, \hat{H}] = -\hbar\omega \hat{a}^\dagger$ . Using these relations, we can get the eigenstates of the Hamiltonian  $\hat{H}$ . We can easily see from the following equations that these eigenstates form a ladder with an energy difference of  $\hbar\omega$ .

$$\begin{aligned}
 \hat{H}|n\rangle &= E_n|n\rangle \\
 \hat{H}\hat{a}|n\rangle &= (\hat{H}\hat{a} - \hat{a}\hat{H} + \hat{a}\hat{H})|n\rangle \\
 &= (E_n - \hbar\omega)\hat{a}|n\rangle
 \end{aligned} \tag{1.5}$$

In the above equations, we see that  $|n\rangle$  is an eigenstate of  $\hat{H}$  with eigenvalue  $E_n$ . We further get the eigenstate of  $\hat{H}$  with eigenvalue  $E_n - \hbar\omega$  by considering the state  $\hat{a}|n\rangle$ . Similarly we see below that  $\hat{a}^\dagger|n\rangle$  also forms the eigenstate of  $\hat{H}$  with eigenvalue  $E_n + \hbar\omega$  for any eigenstate  $|n\rangle$ .

$$\begin{aligned}
 \hat{H}\hat{a}^\dagger|n\rangle &= (E_n + \hbar\omega)\hat{a}^\dagger|n\rangle \\
 \hat{H}|n+1\rangle &= E_{n+1}|n+1\rangle \\
 \hat{H}\hat{a}^\dagger|n+1\rangle &= (E_{n+1} + \hbar\omega)\hat{a}^\dagger|n+1\rangle
 \end{aligned} \tag{1.6}$$

The reason for the terms creation and annihilation operators must be clear from the above equations. It could be loosely said that  $\hat{a}^\dagger$  creates a quantum (or photon) of energy  $\hbar\omega$  and  $\hat{a}$  destroys or annihilates one such quantum of energy or one photon.

There are two important questions that need to be discussed here. The energy cannot be arbitrary negative, but Eq. (1.5) tells us that we can always get a lower energy by using the annihilation operator. The fix is that for the state  $|0\rangle$  corresponding to the minimum energy  $E_0$ ,  $\hat{a}|0\rangle = 0$ . We find that the ground state energy for the quantum harmonic oscillator is non-zero.

$$\begin{aligned}
 \hat{H}|0\rangle &= \hbar\omega \left( \hat{a}^\dagger\hat{a} + \frac{1}{2} \right) |0\rangle = \frac{1}{2}\hbar\omega|0\rangle \\
 E_n &= \hbar\omega \left( n + \frac{1}{2} \right)
 \end{aligned} \tag{1.7}$$

Here  $\hat{a}^\dagger\hat{a} = \hat{n}$  which is the number operator such that  $\hat{n}|n\rangle = n|n\rangle$

The second problem is how do we know that the ladder of energy given by the energy eigenvalues is unique. The resolution, here, is that if we have two such ladders, then there are two different lower bounds and hence two states, which when acted upon by annihilation operator gives us zero, which is not possible due to the linearity of the operators. Furthermore, node theorem tells us that there cannot be degeneracy in one dimension in a bound system. Therefore, the ladder in the Fig. 1.2 is unique. Since the Hamiltonian  $\hat{H}$  is Hermitian, the eigenkets form an orthonormal basis. Using the normalisation  $\langle n|n\rangle = 1$ , we get

$$\begin{aligned}\hat{a}|n\rangle &= \sqrt{n}|n-1\rangle \\ \hat{a}^\dagger|n\rangle &= \sqrt{n+1}|n+1\rangle\end{aligned}\tag{1.8}$$

### Quantum Fluctuations in a field

The number states, that we studied above are also called stationary states. Stationary states are the eigenstates of the Hamiltonian operator and a system in such a state, remains in the same state when subjected to unitary time evolution. The electric field and the magnetic field operators do not commute with the Hamiltonian.

$$\begin{aligned}\hat{E}_x(z, t) &= \left(\frac{2\omega^2}{V\epsilon_0}\right)^{1/2} \hat{q}(t) \sin(kz) \\ &= \sqrt{2}E_0\hat{X}_1(t) \sin(kz) = E_0(\hat{a} + \hat{a}^\dagger) \sin(kz) \\ \hat{B}_y(z, t) &= \left(\frac{\mu_0\epsilon_0}{k}\right) \left(\frac{2\omega^2}{V\epsilon_0}\right)^{1/2} \hat{p}(t) \cos(kz) \\ &= \sqrt{2}B_0\hat{X}_2(t) \cos(kz) = B_0\frac{(\hat{a} - \hat{a}^\dagger)}{i} \cos(kz)\end{aligned}\tag{1.9}$$

Here,  $\hat{X}_1$  and  $\hat{X}_2$  are the quadrature operators from Eq. (1.4). They satisfy the commutation relation  $[\hat{X}_1, \hat{X}_2] = i$ , from which it follows that

$$\langle(\Delta X_1)^2\rangle\langle(\Delta X_2)^2\rangle \geq \frac{1}{4}.\tag{1.10}$$

For the number states,  $\langle n|\hat{X}_1|n\rangle = 0 = \langle n|\hat{X}_2|n\rangle$  but

$$\begin{aligned}\langle n|\hat{X}_1^2|n\rangle &= \frac{1}{2}\langle n|\hat{a}^2 + \hat{a}^{\dagger 2} + \hat{a}^\dagger\hat{a} + \hat{a}\hat{a}^\dagger|n\rangle \\ &= \frac{1}{2}\langle n|\hat{a}^2 + \hat{a}^{\dagger 2} + 2\hat{a}^\dagger\hat{a} + \hat{I}|n\rangle \\ &= \frac{1}{2}(2n+1) = \langle n|\hat{X}_2^2|n\rangle\end{aligned}\tag{1.11}$$

Thus for a number state, the uncertainties in both quadrature are the same and furthermore the vacuum state ( $n=0$ ) minimizes the uncertainty product since

$$\langle(\Delta\hat{X}_1)^2\rangle_{\text{vac}} = \frac{1}{2} = \langle(\Delta\hat{X}_2)^2\rangle_{\text{vac}}\tag{1.12}$$

The quadrature operators in Eq. (1.9) depends upon time. However we can deal with time independent variants of these operators.

$$\begin{aligned}
\frac{d\hat{a}}{dt} &= \frac{i}{\hbar} [\hat{H}, \hat{a}] = -i\omega\hat{a} \\
\hat{a}(t) &= \hat{a}(0)e^{-i\omega t} \\
\hat{a}^\dagger(t) &= \hat{a}^\dagger(0)e^{i\omega t} \\
\hat{X}_1(t) &= \hat{X}_1 \cos \omega t + \hat{X}_2 \sin \omega t \\
\hat{X}_2(t) &= \hat{X}_2 \cos \omega t - \hat{X}_1 \sin \omega t
\end{aligned} \tag{1.13}$$

The time evolution of quadrature operators looks similar to the case of classical harmonic oscillator. The operators  $\hat{q}$  and  $\hat{p}$  (relabelled quadrature operators for convenience) “oscillate” with angular frequency  $\omega$ , just like their classical analogues. But in the case of quantum harmonic oscillator,  $\langle n|\hat{q}|n\rangle = 0 = \langle n|\hat{p}|n\rangle$ . Thus, for the stationary number states, we observe no oscillations. However, we may look at a superposition of these states and a logical question to ask is that which superposition of energy eigenkets imitates the classical oscillator most closely? In the language of wave-function, this implies a wave packet that bounces back and forth without any spread in shape [20]. This job is done a coherent state  $|\alpha\rangle$ , which is an eigenstate of annihilation operator  $\hat{a}$ :

$$\hat{a}|\alpha\rangle = \alpha|\alpha\rangle \tag{1.14}$$

where  $\alpha$  is a complex eigenvalue since  $\hat{a}$  is a non-Hermitian operator. The coherent state can be expressed as a superposition of energy eigenkets.

$$|\alpha\rangle = e^{-|\alpha|^2/2} \sum_{n=0}^{\infty} \frac{\alpha^n}{\sqrt{n!}} |n\rangle \tag{1.15}$$

The probability of detecting  $n$  photons in the coherent state  $|\alpha\rangle$  is given by

$$P_\alpha(n) = |\langle n|\alpha\rangle|^2 \tag{1.16}$$

This is a Poisson distribution about  $|\alpha|^2$  (or mean  $n = \langle \hat{n} \rangle = \langle \alpha|\hat{n}|\alpha\rangle = |\alpha|^2$ ). It is to be noted that although coherent states are normalised, but they are not orthogonal. Their inner product and the completeness can be expressed as follows

$$\begin{aligned}
\langle \alpha|\beta\rangle &= \exp \left[ -\frac{|\alpha|^2}{2} - \frac{|\beta|^2}{2} + \alpha^*\beta \right] \\
\langle \alpha|\alpha\rangle &= 1, \quad \int d^2\alpha |\alpha\rangle \langle \alpha| = \pi \mathbb{I}
\end{aligned} \tag{1.17}$$

They form an over-complete set of states in the Hilbert space [6]. We will deal with coherent states in the later sections. The phase space representation which turns

out to be Gaussian, relation with displacement operator and minimum uncertainty relation makes them an interesting set of states to study.

### 1.1.2 Continuous Variable System

The states of a quantum harmonic oscillator lie in Hilbert space. We have different Hermitian operators in this space e.g. position, momentum [Eq. (1.3)], and number operator [Eq. (1.7)]; which raises the question about dimensions of the Hilbert space. Spectral theorem tells us that a self-adjoint operator has an orthonormal basis of eigenkets [10]. For the position and momentum operator, we get a continuous spectra of functions which are their eigenvectors. Although these eigenvectors are orthonormal in a continuous sense where the Kronecker delta is replaced by a Dirac delta function, they are non-normalizable and these do not lie in the Hilbert space. Therefore, Hilbert space for a quantum harmonic oscillator has countable infinite dimensions corresponding to the number (or fock) basis. The position and momentum operators are called unbounded operators for the above reason and there are multiple ways of dealing with them like considering a rigged Hilbert space [19] or a trick by Weyl that we consider here [4].

#### Weyl Map

We consider Cartesian quantum systems, or the systems whose basic dynamical variables are Cartesian positions and conjugate Cartesian momenta. We can write the state for such a system in position and momentum space [20].

$$\begin{aligned}
 \hat{q}|q\rangle &= q|q\rangle, \quad \hat{p}|p\rangle = p|p\rangle, \quad [q, p] = i\mathbb{I} \\
 |\psi\rangle \in H : \psi(q) &= \langle q|\psi\rangle, \quad \phi(p) = \langle p|\psi\rangle \\
 (\hat{q}\psi)(q) &= q\psi(q), \quad (\hat{p}\psi)(q) = -i\frac{d\psi(q)}{dq} \\
 (\hat{p}\phi)(p) &= p\phi(p), \quad (\hat{q}\phi)(p) = -i\frac{d\phi(p)}{dp} \\
 \phi(p) &= \frac{1}{\sqrt{2\pi}} \int dq e^{-ipq} \psi(q)
 \end{aligned} \tag{1.18}$$

However as discussed earlier, the states that we consider should be normalizable. We can alternatively deal with displacement operators  $D(q, p)$ , which are unitary

operators and have no domain problems.

$$\begin{aligned} D(q, p) &= e^{i(p\hat{q} - q\hat{p})}, \quad -\infty < q, p < \infty \\ D(q, p)^\dagger D(q, p) &= 1 \end{aligned} \quad (1.19)$$

Using Weyl form of commutation relation:  $e^{ip\hat{q}}e^{iq\hat{p}} = e^{ip\hat{q} + iq\hat{p} - \frac{1}{2}iqp} = e^{-iqp}e^{iq\hat{p}}e^{ip\hat{q}}$  (standard, symmetric and anti-standard respectively), we can derive how displacement operator acts upon other states and operators.

$$\begin{aligned} D(q', p')D(q, p) &= e^{\frac{i}{2}(p'q - q'p)} D(q' + q, p' + p) \\ D(q, p)(\hat{q} \text{ or } \hat{p})D(q, p)^{-1} &= \hat{q} - q \text{ or } \hat{p} - p \\ D(q, p)|q'\rangle &= e^{i(q' + \frac{q}{2})p}|q' + q\rangle \\ D(q, p)|p'\rangle &= e^{-i(p' + \frac{p}{2})q}|p' + p\rangle \end{aligned} \quad (1.20)$$

Furthermore, the displacement operators form an orthonormal basis in Hilbert space  $H$ , with respect to the ‘Hilbert-Schmidt inner product’:  $\langle \hat{A} | \hat{B} \rangle = \text{Tr} [\hat{A}^\dagger \hat{B}]$ .

$$\begin{aligned} \text{Tr} [D(q', p')^\dagger D(q, p)] &= \text{Tr} [D(-q', -p')D(q, p)] \\ &= e^{\frac{i}{2}(q'p - p'q)} \text{Tr} [D(q - q', p - p')] \\ &= e^{\frac{i}{2}(q'p - p'q)} \int dx \langle x | D(q - q', p - p') | x \rangle \\ &= e^{\frac{i}{2}(q'p - p'q)} \int dx \langle x | x + q - q' \rangle e^{i(x + \frac{q - q'}{2})(p - p')} \\ &= 2\pi \delta(q - q') \delta(p - p') \end{aligned} \quad (1.21)$$

Now we illustrate the Weyl Map. The dynamical variables for a classical system are real functions  $f(q, p)$ , while for the corresponding quantum system, they are Hermitian operators  $\hat{F}$  acting on the Hilbert space  $H$ . Weyl Map is a rule or a convention that sets up a one-to-one correspondence from  $f(q, p)$  to  $\hat{F}$ .

$$\begin{aligned} q &\rightarrow \hat{q}, \quad p \rightarrow \hat{p}, \quad \sigma q - \tau p \rightarrow \sigma \hat{q} - \tau \hat{p} \\ q^m p^n &= \text{coefficient of } \frac{(m+n)!}{m!n!} \sigma^m (-\tau)^n \text{ in } (\sigma q - \tau p)^{m+n} \\ \rightarrow \widehat{(q^m p^n)} &= \text{coefficient of } \frac{(m+n)!}{m!n!} \sigma^m (-\tau)^n \text{ in } (\sigma \hat{q} - \tau \hat{p})^{m+n} \end{aligned} \quad (1.22)$$



As examples, we have:

$$\begin{aligned}
 q^m &\rightarrow \widehat{(q^m)} = \hat{q}^m ; \\
 q^m p &\rightarrow \widehat{(q^m p)} = \frac{1}{(m+1)} (\hat{q}^m \hat{p} + \hat{q}^{m-1} \hat{p} \hat{q} + \hat{q}^{m-2} \hat{p} \hat{q}^2 + \cdots + \hat{p} \hat{q}^m ; \dots \\
 q^m p^n &\rightarrow \widehat{(q^m p^n)} = \left(\frac{1}{i}\right)^m \left(\frac{1}{-i}\right)^n \frac{\partial^{m+n}}{\partial \sigma^m \partial \tau^n} e^{i(\sigma \hat{q} - \tau \hat{p})} \Big|_{\tau=\sigma=0} ; \dots \\
 p^n &\rightarrow \widehat{(p^n)} = \hat{p}^n
 \end{aligned} \tag{1.23}$$

We can also construct the Inverse Weyl Map. We start by applying Weyl Map on the Fourier integral representation of a classical function  $f(q, p)$  [5].

$$\begin{aligned}
 f(q, p) &= \frac{1}{2\pi} \int \int d\tau d\sigma \tilde{f}(\tau, \sigma) e^{i(\sigma q - \tau p)} \\
 \hat{F} &= \frac{1}{2\pi} \int \int d\tau d\sigma \tilde{f}(\tau, \sigma) e^{i(\sigma \hat{q} - \tau \hat{p})} \\
 &= \frac{1}{2\pi} \int \int d\tau d\sigma \tilde{f}(\tau, \sigma) D(\tau, \sigma)
 \end{aligned} \tag{1.24}$$

Using Eq. (1.19) and (1.22), we can write  $\text{Tr} [D(\tau, \sigma)^\dagger \hat{F}] = \tilde{f}(\tau, \sigma)$ , which seems like an expansion of  $\hat{F}$  in displacement operators' basis. This is also called the quantum operator form of the Fourier integral representation.

$$\hat{F} = \frac{1}{2\pi} \int \int d\tau d\sigma \text{Tr} [D(\tau, \sigma)^\dagger \hat{F}] D(\tau, \sigma) \tag{1.25}$$

Finally, the Inverse Weyl Map which is a one-to-one correspondence from  $\hat{F}$  to  $f(q, p)$  is given as

$$f(q, p) = \frac{1}{2\pi} \int \int d\tau d\sigma \text{Tr} [D(\tau, \sigma)^\dagger \hat{F}] e^{i(\sigma q - \tau p)} \tag{1.26}$$

The Weyl rule gives a one-to-one correspondence between classical phase functions and quantum operators, hence  $f(q, p)$  and  $\hat{F}$  have the same dimensions  $f(q, p) \rightarrow \hat{F} = (f(q, p))_w$ . We now give an important consequence of this rule, along with the Parseval formula, which gives Hilbert-Schmidt inner product of any two operators.

$$\begin{aligned}
 \text{Tr} [\hat{G}^\dagger \hat{F}] &= \frac{1}{2\pi} \int \int d\tau d\sigma \text{Tr} [D(\tau, \sigma)^\dagger \hat{F}] \text{Tr} [\hat{G}^\dagger D(\tau, \sigma)] \\
 &= \frac{1}{2\pi} \int \int d\tau d\sigma \tilde{f}(\tau, \sigma) \tilde{g}(\tau, \sigma)^* \\
 &= \frac{1}{2\pi} \int \int dq dp f(q, p) g(q, p)^*
 \end{aligned} \tag{1.27}$$

Thus, the square integrable functions in the classical phase space are mapped to the operators with finite Hilbert-Schmidt norm by Weyl Rule.

### Phase Space Distribution

The idea of the Wigner distribution  $W(q, p)$  is to express the expectation value of any observable  $\hat{F}$  in a familiar looking form from classical statistical mechanics. Using the formalism developed above, we can write the expectation value of  $\hat{F}$  ( $= [(f(q, p))]_w$ ) for a quantum state with density matrix  $\hat{\rho}$  [24].

$$\begin{aligned}\langle \hat{F} \rangle &= \text{Tr} [\hat{\rho} \hat{F}] \\ &= \int \int dq dp W(q, p) f(q, p) \\ (W(q, p))_w &= \frac{1}{2\pi} \hat{\rho} = (\text{Wigner Distribution})_w\end{aligned}\tag{1.28}$$

The Wigner distribution  $W(q, p)$  is called quasi probability distribution in the phase space because of the reasons that will become clear in the following analysis.

$$\begin{aligned}W(q, p) &= \frac{1}{(2\pi)^2} \int \int d\tau d\sigma \text{Tr} [D(\tau, \sigma)^\dagger \hat{\rho}] e^{i(\sigma q - \tau p)} \\ &= \frac{1}{(2\pi)^2} \int \int d\tau d\sigma \text{Tr} [D(\tau, \sigma) \hat{\rho}] e^{-i(\sigma q - \tau p)} \\ &= \frac{1}{(2\pi)^2} \int \int d\tau d\sigma \int dx \langle x | D(\tau, \sigma) \hat{\rho} | x \rangle e^{-i(\sigma q - \tau p)} \\ &= \frac{1}{(2\pi)^2} \int \int d\tau d\sigma \int dx \langle x | \hat{\rho} | x + \tau \rangle e^{i(x + \frac{\tau}{2})\sigma} e^{-i(\sigma q - \tau p)} \\ &= \frac{1}{2\pi} \int \int d\tau dx e^{i\tau p} \langle x | \hat{\rho} | x + \tau \rangle \delta(x + \frac{\tau}{2} - q) \\ &= \frac{1}{2\pi} \int d\tau e^{ip\tau} \langle q - \frac{\tau}{2} | \hat{\rho} | q + \frac{\tau}{2} \rangle\end{aligned}\tag{1.29}$$

$$\chi_W(\tau, \sigma) = \text{Tr} [D(\tau, \sigma)^\dagger \hat{\rho}]$$

$$\hat{\rho}^\dagger = \hat{\rho} \implies W(q, p) \text{ is real}$$

$$\int \int dq dp W(q, p) = \int dq \langle q | \hat{\rho} | q \rangle = \text{Tr} [\hat{\rho}] = 1$$

$$\hat{\rho} \geq 0 \nRightarrow W(q, p) \geq 0$$

The Wigner characteristic function  $\chi_W(\tau, \sigma)$ , which is a distribution in Fourier transform space of the Wigner function, turns out to be very useful in the next chapter. We further deal with multi-mode fields and hence need to generalise the phase space formalism. For  $n$  Cartesian canonical pairs, we have  $2n$  operators that can be grouped together in a column vector. The canonical commutation relation and Wigner distri-

bution can be defined accordingly.

$$\begin{aligned}
\hat{\xi} = (\hat{\xi}_i) &= (\hat{q}_1, \hat{p}_1, \dots, \hat{q}_n, \hat{p}_n)^T, \quad i = 1, 2, \dots, 2n \\
[\hat{\xi}_i, \hat{\xi}_j] &= i\Omega_{ij}, \quad i, j = 1, 2, \dots, 2n \\
\Omega &= \bigoplus_{k=1}^n \omega, \quad \omega = \begin{pmatrix} 0 & 1 \\ -1 & 0 \end{pmatrix} \\
W(\xi) = W(\vec{q}, \vec{p}) &= \frac{1}{(2\pi)^n} \int_{R^n} d^n \tau \, e^{i\vec{p} \cdot \vec{\tau}} \langle \vec{q} - \frac{\vec{\tau}}{2} | \hat{\rho} | \vec{q} + \frac{\vec{\tau}}{2} \rangle
\end{aligned} \tag{1.30}$$

The direct sum structure of phase space, as seen in the commutator matrix is important. While dealing with the states whose Wigner distribution is Gaussian (Gaussian states), the second moment is represented by a covariance matrix. These matrices also follow a similar direct sum structure for multi-mode systems.

## 1.2 Continuous Variable Teleportation

Quantum teleportation consists of the transfer of an unknown quantum state  $\hat{\rho}_{in}$  from a sender, usually called Alice, to a remote receiver, usually called Bob. This task is accomplished by dividing the information  $\hat{\rho}_{in}$  into two parts: one classical and the other non-classical, and send them to Bob using a classical and a non-classical channel, respectively. The former one can be an email and the latter is a bipartite quantum system with strong long-range correlations. This is an EPR pair or a resource state which is distributed between the sender and receiver in advance. After these transmissions, Bob reconstructs the state  $\hat{\rho}_{out}(= \hat{\rho}_{in}$  ideally) by acting on the quantum channel and the original state at Alice's is destroyed during the process. The net result of the quantum teleportation is the removal of the original state  $\hat{\rho}_A$  from Alice's and its appearance in Bob's lab after some time. This time is limited by the classical channel [2].

The original protocol for quantum teleportation or discrete variable quantum teleportation uses bipartite qubit resource states and Bell measurements in order to couple Alice's input qubit state with the quantum channel. On the other hand, continuous variable quantum teleportation uses linear passive optics and homodyne measurements in its protocol.

### 1.2.1 Teleportation using TMSV state

Quantum correlation or entanglement in the states is the key resource for implementation of quantum information and communication protocols. The techniques developed in quantum optical set-ups to achieve squeezed light makes these correlations comparatively accessible with optical quantum continuous variables [21].

The analogue of a maximally entangled state in infinite dimensions is not normalizable, however it can be approached by a limiting sequence of normalizable states. The state for this job is a two-mode squeezed vacuum (TMSV) state obtained by ideal, noiseless degenerate parametric down conversion processes. It can be constructed by applying a squeezing operation, which is a Gaussian operation (an operation that preserves the Gaussianity of the Wigner function) on a vacuum state (a Gaussian state centred at origin in phase space) and then operation of a balanced beam-splitter on two such states. At the limit of squeezing parameter  $r \rightarrow \infty$ , it approaches a maximally entangled state.

#### Protocol for teleportation of a Gaussian state

Alice and Bob share a two-mode squeezed vacuum (TMSV) state with squeezing parameter  $r$ . Alice wants to send an unknown Gaussian state C to Bob: first and second moments of C are  $\mathbf{r}_0$  and  $\sigma_0$  respectively. The initial Gaussian state in order B, A, C is given by first moment  $\mu_{BAC}$  and second moment  $V_{BAC}$ :

$$\begin{pmatrix} 0 \\ 0 \\ \mathbf{r}_0 \end{pmatrix}, \begin{pmatrix} \cosh(2r)\mathbb{I}_2 & \sinh(2r)\sigma_z & 0 \\ \sinh(2r)\sigma_z & \cosh(2r)\mathbb{I}_2 & 0 \\ 0 & 0 & \sigma_0 \end{pmatrix} \quad (1.31)$$

Alice projects the system AC to the following two-mode squeezed state, given by  $\mu_{A'C'}$  and  $V_{A'C'}$ :

$$\begin{pmatrix} 0 \\ \mathbf{r} \end{pmatrix}, \begin{pmatrix} \cosh(2r')\mathbb{I}_2 & \sinh(2r')\sigma_z \\ \sinh(2r')\sigma_z & \cosh(2r')\mathbb{I}_2 \end{pmatrix} \quad (1.32)$$

Here, Gaussian states have been represented by their first and second moments only. The Wigner function and Wigner characteristic function for Gaussian states with mean vector  $\mu$  and covariance matrix  $V$  are given by

$$\begin{aligned} W(\xi) &= \frac{\exp[-(1/2)(\xi - \mu)^T V^{-1}(\xi - \mu)]}{2\pi\sqrt{\det V}} \\ \chi(\Lambda) &= \exp\left[-\frac{1}{2}\Lambda^T(\Omega V \Omega^T)\Lambda - i(\Omega\mu)^T \Lambda\right] \end{aligned} \quad (1.33)$$

The projection by Alice is achieved by a double-homodyne measurement. The experimental details can be found in the reference [17]. We can use general-dyne filtering calculations [21] to find Bob's state after this measurement.

$$\begin{aligned}
W_B &= \frac{\int W_{BAC} W_{A'C'} dx_A dp_A dx_C dp_C}{\int W_{BAC} W_{A'C'} dx_B dp_B dx_A dp_A dx_C dp_C} \\
\mathbf{r}_B &= -\sinh(2r) [\cosh(2r) \mathbb{I}_2 + \sigma_0]^{-1} (\mathbf{r} - \mathbf{r}_0) \\
\sigma_B &= \cosh(2r) \mathbb{I}_2 - [\sinh(2r)]^2 [\cosh(2r) \mathbb{I}_2 + \sigma_0]^{-1}
\end{aligned} \tag{1.34}$$

We have used the approximation  $r' \rightarrow \infty$  during the measurement. Further, the measurement outcome  $\mathbf{r}$  is sent to Bob by a classical channel. Bob does a feed-forward unitary operation on his state depending upon  $\mathbf{r}$ .

$$\begin{aligned}
\mathbf{r}_B &= -\sinh(2r) [\cosh(2r) \mathbb{I}_2 + \sigma_0]^{-1} (\mathbf{r} - \mathbf{r}_0) + \mathbf{f}(\mathbf{r}) \\
\sigma_B &= \cosh(2r) \mathbb{I}_2 - [\sinh(2r)]^2 [\cosh(2r) \mathbb{I}_2 + \sigma_0]^{-1}
\end{aligned} \tag{1.35}$$

The fidelity can be optimised with respect to  $\mathbf{f}(\mathbf{r})$  to get a maximum value. However, throughout our calculations, we assume  $\mathbf{f}(\mathbf{r}) = \mathbf{r}$  (the optimal feed-forward for the case of maximally entangled resource).

### Calculations using Wigner Characteristic Function

Before doing the fidelity calculations, we give here an alternative approach using Wigner characteristic functions for teleportation of a Gaussian state (specifically, coherent state) using TMSV state as the resource state [13].

$$\begin{aligned}
\chi_{in} &= e^{-\frac{1}{4}(\tau^2 + \sigma^2)} e^{-i(\tau\sigma_0 - \sigma\tau_0)} = \chi_{\text{coherent}} \\
\chi_{\text{EPR}}(\Lambda_1, \Lambda_2) &= \chi_{\text{EPR}}(\tau_1, \sigma_1, \tau_2, \sigma_2) = \chi_{\text{TMSV}} \\
&= e^{-\frac{1}{4}(\tau_1^2 + \sigma_1^2 + \tau_2^2 + \sigma_2^2)} \cosh(2r) e^{-\frac{1}{2}(\sigma_1\sigma_2 - \tau_1\tau_2) \sinh(2r)} \\
\chi_{out}(\tau, \sigma) &= \chi_{in}(\tau, \sigma) \chi_{\text{EPR}}(\tau, -\sigma, \tau, \sigma) \\
&= \left[ e^{-\frac{1}{4}(\tau^2 + \sigma^2)} e^{-i(\tau\sigma_0 - \sigma\tau_0)} \right] \left[ e^{-\frac{1}{2}(\tau^2 + \sigma^2) \cosh(2r)} \right] \\
&\quad \times \left[ e^{\frac{1}{2}(\sigma^2 + \tau^2) \sinh(2r)} \right] \\
&= \exp \left[ -\frac{2e^{-2r} + 1}{4} (\tau^2 + \sigma^2) - i\tau\sigma_0 + i\sigma\tau_0 \right]
\end{aligned} \tag{1.36}$$

$$\begin{aligned}
\text{Fidelity (F)} &= \frac{1}{2\pi} \int \int d\tau d\sigma \chi_{in}(\tau, \sigma) \chi_{out}(-\tau, -\sigma) \\
&= \frac{1}{2\pi} \int \int d\tau d\sigma \left[ e^{-\frac{1}{4}(\tau^2 + \sigma^2)} e^{-i(\tau\sigma_0 - \sigma\tau_0)} \right] \\
&\quad \times \exp \left[ -\frac{2e^{-2r} + 1}{4} (\tau^2 + \sigma^2) + i\tau\sigma_0 - i\sigma\tau_0 \right] \quad (1.37) \\
&= \frac{1}{2\pi} \int \int d\tau d\sigma \exp \left[ -\frac{e^{-2r} + 1}{2} (\tau^2 + \sigma^2) \right] \\
&= \frac{1}{e^{-2r} + 1}
\end{aligned}$$

This is the fidelity that will be used as reference in the future calculations. The fidelity of teleportation for the case of different non-Gaussian resource states is compared to the above expression.



## Chapter 2

# Non-Gaussian Operations on two-mode squeezed Coherent State

### 2.1 Non-Gaussian operations on one mode

The teleportation protocol considered in the last chapter considers only Gaussian states: vacuum state is a Gaussian state centered at the origin of the phase space with minimum (symmetric) quadrature uncertainty and coherent state is a displaced vacuum state; and the double homodyne measurement, which is a Gaussian measurement. The squeezed states are Gaussian states where the canonical quadrature have uncertainties below the vacuum noise (still respecting the total uncertainty  $\Delta x \Delta p = 1/2$ ).

However, Gaussian states are often criticized for the fact that the statistics obtained from Gaussian measurements on these states can be reproduced by classical probability distributions [21]. There exist non-Gaussian states like other fock states and photon subtracted squeezed states that we consider in this section. We expect that introducing non-Gaussianity in the entangled squeezed states can give stronger correlations. Here we consider a non-Gaussian operation on one of the modes of a two mode squeezed coherent state.

#### Protocol

As discussed in the previous chapter, the Wigner characteristic function for a Gaussian state with mean vector  $\mu$  and covariance matrix  $V$  is given by

$$\chi(\Lambda) = \exp\left[-\frac{1}{2}\Lambda^T(\Omega V \Omega^T)\Lambda - i(\Omega\mu)^T\Lambda\right] \quad (2.1)$$

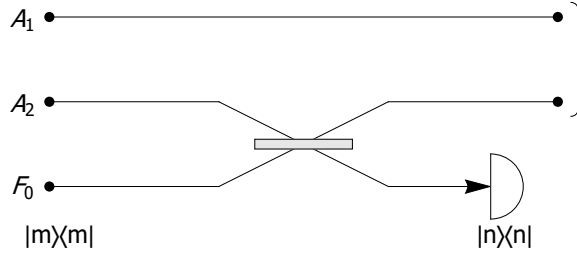


Figure 2.1: Schematic for non-Gaussian operation on one of the modes of two mode squeezed coherent (TMSC) state.

We can compute the Wigner characteristic function of a two-mode coherent state, which comes out to be the product of the Wigner characteristic function of two single-mode coherent states because of the direct sum structure of the phase space. We can assume the same displacement for both modes ( $d_1 = d$ ,  $d_2 = 0$ ).

$$\begin{aligned}\chi(\tau_1, \sigma_1, \tau_2, \sigma_2) &= e^{-(1/4)(\tau_1^2 + \sigma_1^2)} e^{-i(\tau_1 d_2 - \sigma_1 d_1)} e^{-(1/4)(\tau_2^2 + \sigma_2^2)} e^{-i(\tau_2 d_2 - \sigma_2 d_1)} \\ &= e^{-(1/4)(\tau_1^2 + \sigma_1^2)} e^{i\sigma_1 d} e^{-(1/4)(\tau_2^2 + \sigma_2^2)} e^{i\sigma_2 d}\end{aligned}\quad (2.2)$$

The two mode squeezed coherent state can be obtained by applying the two mode squeezing operation  $S_{12}$  on the quadrature. The characteristic function changes as  $\chi(\Lambda) \rightarrow \chi(S_{12}^{-1}\Lambda)$ .

$$\begin{aligned}\begin{pmatrix} \tau_1 \\ \sigma_1 \\ \tau_2 \\ \sigma_2 \end{pmatrix} &\xrightarrow{S_{12}^{-1}(r)} \begin{pmatrix} \cosh r \mathbb{I} & \sinh r \mathbb{Z} \\ \sinh r \mathbb{Z} & \cosh r \mathbb{I} \end{pmatrix}^{-1} \begin{pmatrix} \tau_1 \\ \sigma_1 \\ \tau_2 \\ \sigma_2 \end{pmatrix} \\ \chi_{\text{TMSC}} &= \exp \left[ -\frac{\tau_1^2 + \sigma_1^2 + \tau_2^2 + \sigma_2^2}{4} \cosh(2r) \right] \\ &\quad \times \exp \left[ \frac{\tau_1 \tau_2 - \sigma_1 \sigma_2}{2} \sinh(2r) + i(\sigma_1 + \sigma_2) d e^r \right] \\ &= \chi_{A_1 A_2}(\tau_1, \sigma_1, \tau_2, \sigma_2)\end{aligned}\quad (2.3)$$

We mix the mode  $A_2$  of the TMSC state, with an auxiliary mode  $F_0$ , initiated to fock state  $|m\rangle\langle m|$  as given in the Fig. 2.1 using a beam-splitter of transmissivity  $T$ . We write the characteristic function for a fock state in terms of Laguerre Polynomial  $L_m$  here.

$$\chi_{|m\rangle}(\tau, \sigma) = \exp \left( -\frac{\tau^2}{4} - \frac{\sigma^2}{4} \right) L_m \left( \frac{\tau^2}{2} + \frac{\sigma^2}{2} \right)$$

The characteristic function post the beam-splitter operation  $B_{23}$  can be calculated in a similar fashion as above.

$$\begin{aligned}
\chi_{A_1 A_2 F_0}(\Lambda) &= \chi_{A_1 A_2}(\tau_1, \sigma_1, \tau_2, \sigma_2) \chi_{|m\rangle}(\tau_3, \sigma_3) \\
&= e^{-\left(\frac{\tau_1^2}{4} + \frac{\sigma_1^2}{4}\right)} e^{-\left(\frac{\tau_2^2}{4} + \frac{\sigma_2^2}{4}\right)} e^{i(\sigma_1 + \sigma_2)d} \\
&\quad \times e^{-\left(\frac{\tau_3^2}{4} + \frac{\sigma_3^2}{4}\right)} L_m\left(\frac{\tau_3^2}{2} + \frac{\sigma_3^2}{2}\right) \\
&\quad \begin{pmatrix} \Lambda_1 \\ \Lambda_2 \\ \Lambda_3 \end{pmatrix} \xrightarrow{B_{23}^{-1}(T)} \begin{pmatrix} \mathbb{I} & 0 & 0 \\ 0 & \sqrt{T} \mathbb{I} & \sqrt{1-T} \mathbb{I} \\ 0 & -\sqrt{1-T} \mathbb{I} & \sqrt{T} \mathbb{I} \end{pmatrix}^{-1} \begin{pmatrix} \Lambda_1 \\ \Lambda_2 \\ \Lambda_3 \end{pmatrix} \\
\chi_{A_1 A_2 F_0}(\Lambda) &\xrightarrow{B_{23}(T)} \chi_{A_1 A'_2 F'_0}(\Lambda) = \chi_{A_1 A'_2 F'_0}(\tau_1, \sigma_1, \tau_2, \sigma_2, \tau_3, \sigma_3)
\end{aligned} \tag{2.4}$$

We project one of the modes that comes out of the beam splitter on the fock basis  $|n\rangle\langle n|$ . The final two mode state obtained is the resultant of the two mode squeezed coherent (TMSC) state post the above non-Gaussian operation on one of its modes. We can compute the unnormalised Wigner characteristic function for this non-Gaussian state.

$$\begin{aligned}
\chi_{A_1 A'_2}(\Lambda_1, \Lambda_2) &= \frac{1}{2\pi} \int d\tau_3 d\sigma_3 \underbrace{\chi_{A_1 A'_2 F'_0}(\tau_1, \sigma_1, \tau_2, \sigma_2, \tau_3, \sigma_3)}_{\text{Three mode entangled state}} \underbrace{\chi_{|n\rangle}(\tau_3, \sigma_3)}_{\text{Projection on } |n\rangle\langle n|} \\
k! L_k\left(\frac{\tau^2}{2} + \frac{\sigma^2}{2}\right) &= \partial_s^k \partial_t^k \exp\left[st + s\frac{\tau + i\sigma}{\sqrt{2}} - t\frac{\tau - i\sigma}{\sqrt{2}}\right] \Big|_{s=t=0}
\end{aligned} \tag{2.5}$$

The unnormalised Wigner characteristic function can be converted into a Gaussian integral using a substitution of generating functions for the Laguerre Polynomials.

## Results

The unnormalised Wigner characteristic function post one mode non-Gaussian operation on the TMSC state comes out to be

$$\begin{aligned}
\chi_{A_1 A'_2}(\tau_1, \sigma_1, \tau_2, \sigma_2) &= \frac{1}{1 - \alpha^2(T - 1)} \partial_{s_1}^m \partial_{t_1}^m \partial_{s_3}^n \partial_{t_3}^n e^{[a_1 s_1 + a_2 t_1 + a_3 s_3 + a_4 t_3]} \\
&\quad \times e^{[a_5 s_1 t_1 + a_6 s_3 t_3 + a_7 (s_3 t_1 + s_1 t_3)]} \Big|_{s_1=t_1=s_3=t_3=0}
\end{aligned} \tag{2.6}$$

The coefficients in the above expression are listed below. The  $F_0$  state which is the fock state  $|m\rangle\langle m|$  is written in Laguerre Polynomials substitution using the variables

$s_1$  and  $t_1$ , whereas the projection operator  $|n\rangle\langle n|$  uses the variables  $s_3$  and  $t_3$ .

$$\begin{aligned}
 a_1 &= \frac{[(-\tau_2(1+\alpha^2) - i\sigma_2(1+\alpha^2) + [(\tau_1 - i\sigma_1)\alpha\sqrt{1+\alpha^2} - d(\alpha + \sqrt{1+\alpha^2})]\sqrt{T})\sqrt{1-T}]}{\sqrt{2}[\alpha^2(T-1) - 1]} \\
 a_2 &= \frac{((\tau_2(1+\alpha^2) - i\sigma_2(1+\alpha^2) - ((\tau_1 + i\sigma_1)\alpha\sqrt{1+\alpha^2} + d(\alpha + \sqrt{1+\alpha^2}))\sqrt{T})\sqrt{1-T})}{(\sqrt{2}(-1 + \alpha^2(T-1)))} \\
 a_3 &= \frac{((d(\alpha + \sqrt{1+\alpha^2}) + \alpha(-(\tau_1 - i\sigma_1)\sqrt{1+\alpha^2} + (\tau_2 + i\sigma_2)\alpha\sqrt{T}))\sqrt{1-T})}{(\sqrt{2}(-1 + \alpha^2(T-1)))} \\
 a_4 &= \frac{((-d(\alpha + \sqrt{1+\alpha^2}) + \alpha(-(\tau_1 + i\sigma_1)\sqrt{1+\alpha^2} + (\tau_2 - i\sigma_2)\alpha\sqrt{T}))\sqrt{1-T})}{(\sqrt{2}(-1 + \alpha^2(T-1)))} \\
 a_5 &= \frac{(1+\alpha^2)(T-1)}{-1 + \alpha^2(T-1)} \quad a_6 = 1 + \frac{1}{-1 + \alpha^2(T-1)} \quad a_7 = \frac{\sqrt{T}}{-1 + \alpha^2(T-1)}
 \end{aligned} \tag{2.7}$$

In these expressions,  $T$  is transmissivity of the beam splitter,  $d$  is the displacement of the coherent state as defined earlier and  $\alpha = \sinh(r)$ . We can give the normalised characteristic function by dividing the unnormalised function by the given probability  $P$  such that  $\chi_{\text{Final}} = \chi_{A_1 A'_2} / P$ .

$$\begin{aligned}
 P &= \chi_{A_1 A'_2}(\Lambda_1, \Lambda_2) \Big|_{\tau_1=\sigma_1=\tau_2=\sigma_2=0} \\
 &= \frac{1}{1 - \alpha^2(\tau - 1)} \partial_{s_1}^m \partial_{t_1}^m \partial_{s_3}^n \partial_{t_3}^n e^{[b_1 s_1 + b_1 t_1 + b_2 s_3 + b_2 t_3]} \\
 &\quad \times e^{[b_3 s_1 t_1 + b_4 s_3 t_3 + b_5 (s_3 t_1 + s_1 t_3)]} \Big|_{s_1=t_1=s_3=t_3=0}
 \end{aligned} \tag{2.8}$$

The coefficients in the above equations have the following expressions:

$$\begin{aligned}
 b_1 &= -\frac{(\sqrt{2}d(\alpha + \sqrt{1+\alpha^2})\sqrt{-(T-1)T})}{(-2 + 2\alpha^2(T-1))} \quad b_2 = -\frac{(d(\alpha + \sqrt{1+\alpha^2})\sqrt{2-2T})}{(-2 + 2\alpha^2(T-1))} \\
 b_3 &= \frac{(1+\alpha^2)(T-1)}{-1 + \alpha^2(T-1)} \quad b_4 = 1 + \frac{1}{-1 + \alpha^2(T-1)} \quad b_5 = \frac{\sqrt{T}}{-1 + \alpha^2(T-1)}
 \end{aligned} \tag{2.9}$$

We can write the above expression back in the original form expressed as the Laguerre Polynomials. However, given the non-triviality of the task, we leave this for the next draft of the document.

## 2.2 Non-Gaussian operations on both modes

Now we consider four modes for the non-Gaussian operation as given in the Fig. 2.2:  $A_1$ ,  $A_2$ ,  $F_0$  and  $F_1$  respectively.

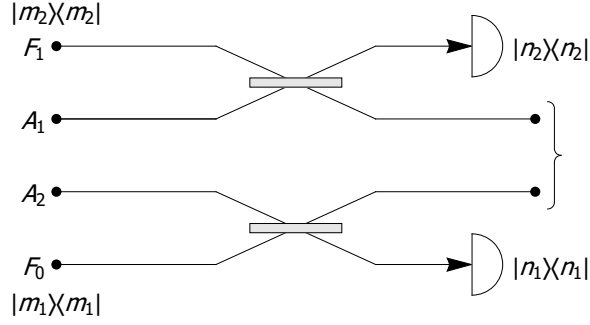


Figure 2.2: Schematic for non-Gaussian operation on both of the modes of two mode squeezed coherent (TMSC) state.

## Protocol

We recall the Wigner characteristic function of two-mode squeezed coherent state and again mix its mode  $A_2$  with auxiliary mode  $F_0$ , a fock state  $|m_1\rangle\langle m_1|$  using the beam-splitter  $B_{23}$  of transmissivity  $T$ . But this time, we also mix the second mode  $A_1$  of TMSC state with an auxiliary mode  $F_1$ , a fock state  $|m_2\rangle\langle m_2|$  using another beam-splitter  $B_{14}$  of transmissivity  $T$ , as shown in the Fig. 2.2. We write the characteristic function of the state post beam-splitter as below.

$$\begin{aligned}
 \chi_{A_1 A_2 F_0 F_1}(\Lambda) &= \chi_{A_1 A_2}(\tau_1, \sigma_1, \tau_2, \sigma_2) \chi_{|m_1\rangle}(\tau_3, \sigma_3) \chi_{|m_2\rangle}(\tau_4, \sigma_4) \\
 &= e^{-\left(\frac{\tau_1^2}{4} + \frac{\sigma_1^2}{4}\right)} e^{-\left(\frac{\tau_2^2}{4} + \frac{\sigma_2^2}{4}\right)} e^{i(\sigma_1 + \sigma_2)d} e^{-\left(\frac{\tau_3^2}{4} + \frac{\sigma_3^2}{4}\right)} \\
 &\quad \times L_{m_1}\left(\frac{\tau_3^2}{2} + \frac{\sigma_3^2}{2}\right) e^{-\left(\frac{\tau_4^2}{4} + \frac{\sigma_4^2}{4}\right)} L_{m_2}\left(\frac{\tau_4^2}{2} + \frac{\sigma_4^2}{2}\right) \\
 \chi_{A_1 A_2 F_0 F_1}(\Lambda) &\xrightarrow{B_{14} \oplus B_{23}} \chi_{A'_1 A'_2 F'_0 F'_1}(\tau_1, \sigma_1, \tau_2, \sigma_2, \tau_3, \sigma_3, \tau_4, \sigma_4)
 \end{aligned} \tag{2.10}$$

We project one of the modes that comes out of the beam splitter  $B_{23}$  on the fock basis  $|n_1\rangle\langle n_1|$  and that comes out of the beam splitter  $B_{14}$  on the fock basis  $|n_2\rangle\langle n_2|$ . The final two mode state obtained is the resultant of the two mode squeezed coherent (TMSC) state post the above non-Gaussian operation on both of its modes. We can

compute the unnormalised Wigner characteristic function for this non-Gaussian state.

$$\begin{aligned}
 \chi_{A'_1 A'_2}(\Lambda_1, \Lambda_2) &= \frac{1}{(2\pi)^2} \int d\tau_3 d\sigma_3 d\tau_4 d\sigma_4 \underbrace{\chi_{A'_1 A'_2 F'_0 F'_1}(\tau_1, \sigma_1, \tau_2, \sigma_2, \tau_3, \sigma_3, \tau_4, \sigma_4)}_{\text{Four mode entangled state}} \\
 &\quad \times \underbrace{\chi_{|n_1\rangle}(\tau_3, \sigma_3)}_{\text{Projecting } F'_0 \text{ on } |n_1\rangle\langle n_1|} \underbrace{\chi_{|n_2\rangle}(\tau_4, \sigma_4)}_{\text{Projecting } F'_1 \text{ on } |n_2\rangle\langle n_2|} \\
 k! L_k \left( \frac{\tau^2}{2} + \frac{\sigma^2}{2} \right) &= \partial_s^k \partial_t^k \exp \left[ st + s \frac{\tau + i\sigma}{\sqrt{2}} - t \frac{\tau - i\sigma}{\sqrt{2}} \right] \Big|_{s=t=0}
 \end{aligned} \tag{2.11}$$

The unnormalised Wigner characteristic function can be converted into a Gaussian integral using the substitution of generating functions for the Laguerre Polynomials.

## Results

The unnormalised Wigner characteristic function post two mode non-Gaussian operation on the TMSC state comes out to be

$$\begin{aligned}
 \chi_{A'_1 A'_2}(\tau_1, \sigma_1, \tau_2, \sigma_2) &= \frac{1}{1 - \alpha^2(T^2 - 1)} \partial_{s_1}^{m_1} \partial_{t_1}^{m_1} \partial_{s_3}^{n_1} \partial_{t_3}^{n_1} \partial_{s_2}^{m_2} \partial_{t_2}^{m_2} \partial_{s_4}^{n_2} \partial_{t_4}^{n_2} \\
 &\quad \times e^{[a_1 s_1 + a_2 t_1 + a_3 s_2 + a_4 t_2 + a_5 s_3 + a_6 t_3 + a_7 s_4 + a_8 t_4 + b_1(s_1 t_1 + s_2 t_2) + b_2(s_3 t_3 + s_4 t_4)]} \\
 &\quad \times e^{[b_3(s_1 s_2 + t_1 t_2) + b_4(s_2 s_3 + s_1 s_4 + t_2 t_3 + t_1 t_4) + b_5(s_3 s_4 + t_3 t_4)]} \\
 &\quad \times e^{[b_6(s_1 t_3 + s_2 t_4 + s_3 t_1 + s_4 t_2)]} \Big|_{s_1=t_1=s_2=t_2=s_3=t_3=s_4=t_4=0}
 \end{aligned} \tag{2.12}$$

$$\begin{aligned}
 a_1 &= - \frac{(\sqrt{1-T}(\tau_2(1+\alpha^2) + i\sigma_2(1+\alpha^2) + \sqrt{1+\alpha^2}(d\sqrt{T} - (\tau_1 - i\sigma_1)\alpha T) + d\alpha T^{3/2}))}{(\sqrt{2}(-1 + \alpha^2(T^2 - 1)))} \\
 a_2 &= - \frac{(\sqrt{1-T}(-\tau_2(1+\alpha^2) + i\sigma_2(1+\alpha^2) + \sqrt{1+\alpha^2}(d\sqrt{T} + (\tau_1 - i\sigma_1)\alpha T) + d\alpha T^{3/2}))}{(\sqrt{2}(-1 + \alpha^2(T^2 - 1)))} \\
 a_3 &= - \frac{(\sqrt{1-T}(\tau_1(1+\alpha^2) + i\sigma_1(1+\alpha^2) + \sqrt{1+\alpha^2}(d\sqrt{T} - (\tau_2 - i\sigma_2)\alpha T) + d\alpha T^{3/2}))}{(\sqrt{2}(-1 + \alpha^2(T^2 - 1)))} \\
 a_4 &= - \frac{(\sqrt{1-T}(-\tau_1(1+\alpha^2) + i\sigma_1(1+\alpha^2) + \sqrt{1+\alpha^2}(d\sqrt{T} + (\tau_2 - i\sigma_2)\alpha T) + d\alpha T^{3/2}))}{(\sqrt{2}(-1 + \alpha^2(T^2 - 1)))}
 \end{aligned} \tag{2.13}$$

$$\begin{aligned}
 a_5 &= - \frac{(\sqrt{1-T}(d(\sqrt{1+\alpha^2} + \alpha T) + \alpha\sqrt{T}(-(\tau_1 - i\sigma_1)\sqrt{1+\alpha^2} + (\tau_2 + i\sigma_2)\alpha\sqrt{T})))}{(\sqrt{2}(-1 + \alpha^2(T^2 - 1)))} \\
 a_6 &= - \frac{(\sqrt{1-T}(d(\sqrt{1+\alpha^2} + \alpha T) + \alpha\sqrt{T}((\tau_1 + i\sigma_1)\sqrt{1+\alpha^2} - (\tau_2 - i\sigma_2)\alpha\sqrt{T})))}{(\sqrt{2}(-1 + \alpha^2(T^2 - 1)))} \\
 a_7 &= - \frac{(\sqrt{1-T}(d(\sqrt{1+\alpha^2} + \alpha T) + \alpha\sqrt{T}(-(\tau_2 - i\sigma_2)\sqrt{1+\alpha^2} + (\tau_1 + i\sigma_1)\alpha\sqrt{T})))}{(\sqrt{2}(-1 + \alpha^2(T^2 - 1)))} \\
 a_8 &= - \frac{(\sqrt{1-T}(d(\sqrt{1+\alpha^2} + \alpha T) + \alpha\sqrt{T}((\tau_2 + i\sigma_2)\sqrt{1+\alpha^2} - (\tau_1 - i\sigma_1)\alpha\sqrt{T})))}{(\sqrt{2}(-1 + \alpha^2(T^2 - 1)))} \\
 b_1 &= \frac{(1 + \alpha^2)(T - 1)}{-1 + \alpha^2(T^2 - 1)} \quad b_2 = \frac{\alpha^2(T - 1)T}{-1 + \alpha^2(T^2 - 1)} \quad b_3 = \frac{\alpha\sqrt{1+\alpha^2}(T - 1)T}{-1 + \alpha^2(T^2 - 1)} \\
 b_4 &= \frac{\alpha\sqrt{1+\alpha^2}(T - 1)\sqrt{T}}{-1 + \alpha^2(T^2 - 1)} \quad b_5 = \frac{\alpha\sqrt{1+\alpha^2}(T - 1)}{-1 + \alpha^2(T^2 - 1)} \quad b_6 = \frac{(-1 + \alpha^2(T - 1))\sqrt{T}}{-1 + \alpha^2(T^2 - 1)}
 \end{aligned} \tag{2.14}$$

In these expressions,  $T$  is transmissivity of the beam splitter,  $d$  is the displacement of the coherent state as defined earlier and  $\alpha = \sinh(r)$ . We can give the normalised characteristic function by dividing the unnormalised function by the given probability  $P$  such that  $\chi_{\text{Final}} = \chi_{A'_1 A'_2} / P$ .

$$\begin{aligned}
 P &= \chi_{A'_1 A'_2}(\Lambda_1, \Lambda_2) \Big|_{\tau_1=\sigma_1=\tau_2=\sigma_2=0} \\
 &= \frac{1}{1 - \alpha^2(T^2 - 1)} \partial_{s_1}^{m_1} \partial_{t_1}^{m_1} \partial_{s_3}^{n_1} \partial_{t_3}^{n_1} \partial_{s_2}^{m_2} \partial_{t_2}^{m_2} \partial_{s_4}^{n_2} \partial_{t_4}^{n_2} \\
 &\quad \times e^{[c_0 + c_1(s_1+t_1+s_2+t_2) + c_2(s_3+t_3+s_4+t_4) + b_1(s_1 t_1 + s_2 t_2)]} \\
 &\quad \times e^{[b_2(s_3 t_3 + s_4 t_4) + b_3(s_1 s_2 + t_1 t_2) + b_4(s_2 s_3 + s_1 s_4 + t_2 t_3 + t_1 t_4)]} \\
 &\quad \times e^{[b_5(s_3 s_4 + t_3 t_4) + b_6(s_1 t_3 + s_2 t_4 + s_3 t_1 + s_4 t_2)]} \Big|_{s_1=t_1=s_2=t_2=s_3=t_3=s_4=t_4=0}
 \end{aligned} \tag{2.15}$$

The other coefficients used in the above equations have the following expressions:

$$\begin{aligned}
 b_7 &= - \frac{(d^2(T - 1)(1 + \alpha(\alpha + \sqrt{1 + \alpha^2}(1 + T))))}{(-1 + \alpha^2(T^2 - 1))} \\
 b_8 &= - \frac{(d\sqrt{-(T - 1)T}(\sqrt{1 + \alpha^2} + \alpha T))}{(\sqrt{2}(-1 + \alpha^2(T^2 - 1)))} \\
 b_9 &= - \frac{d\sqrt{2 - 2T}(\sqrt{1 + \alpha^2} + \alpha T)}{-2 + 2\alpha^2(T^2 - 1)}
 \end{aligned} \tag{2.16}$$

The teleportation fidelity and output state calculations to be done in the next chapter relies on the Wigner characteristic function formalism. The resource states considered

in this chapter will be used for those protocols. The expressions for the Wigner characteristic function derived here are in the general form, for a variable  $|m\rangle\langle m|$  and a random detector  $|n\rangle\langle n|$ . Different types of non-Gaussian operations arise for different values of these variables as we shall see in the next chapter.



## Chapter 3

# Non-Gaussian Resource States in Continuous Variable Quantum Teleportation

The resource states in this chapter (two mode squeezed coherent states) represent the set of Gaussian pure states with minimum (symmetric) uncertainty in the phase space, characterised by the displacement  $d$ . The generalised non-Gaussian operations, defined in the previous chapter, are used on the two mode squeezed coherent (TMSC) state in the given manner:

- Photon Subtraction on TMSC ( $m = 0$ ), ( $n = 1, 2$ )
- Photon Addition on TMSC ( $m = 1, 2$ ), ( $n = 0$ )
- Photon Catalysis on TMSC ( $m = n$ ), ( $n = 1, 2$ )

### 3.1 Asymmetric Case

If the non-Gaussian operation is done on one of the modes of the TMSC state and it is used as a resource for teleportation of a Gaussian state, we get the Asymmetric case. The fidelity for different non-Gaussian operations is given as individual cases below.

#### 3.1.1 Photon Subtraction on one mode of TMSC state

In this case, we take  $m = 0$  and  $n = 1$  in the Fig. 2.1. One photon is subtracted from the two mode squeezed coherent state at the output. The output state is called

one-photon subtracted two mode squeezed coherent (1-PSTMSC) state. The characteristic function can be found by putting the appropriate values of  $m$  and  $n$  in the Eq. (2.6). Further we use Eq. (1.36) and (1.37) to get the fidelity of teleportation. The expressions for the fidelity are too complicated and long to be included in this document therefore we directly provide the plots of the Fidelity ( $F$ ) with respect to squeezing parameter ( $r$ ). Higher  $r$  represents higher entanglement between the two modes of the squeezed state. Since, the resource state represents a family of states

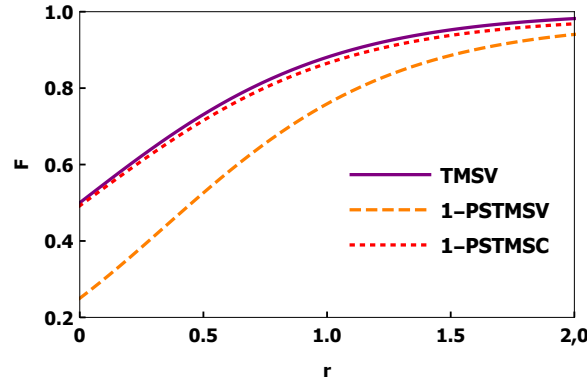


Figure 3.1: Fidelity ( $F$ ) vs squeezing parameter ( $r$ ) of teleportation for one-photon-subtracted two mode squeezed coherent (1-PSTMSC) state.

which is characterised by  $d$ , we can also plot Fidelity ( $F$ ) for different displacements ( $d$ ) which shows a trend for different state functions in phase space. As seen in the

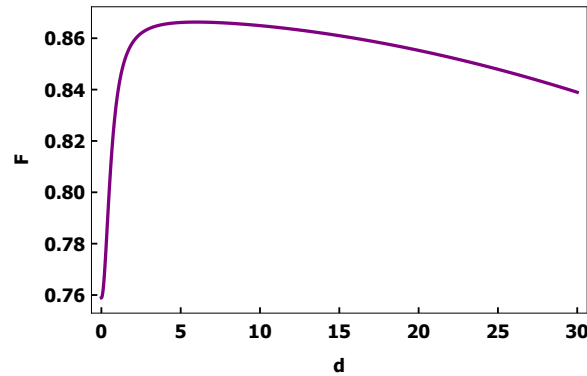


Figure 3.2: Fidelity ( $F$ ) vs displacement ( $d$ ) of teleportation for one-photon-subtracted two mode squeezed coherent (1-PSTMSC) state.

trends above, the fidelity increases initially as we move away from the origin of phase space, then for higher displacements it starts decreasing. The graph is drawn for the

fixed squeezing parameter  $r = 1$ . Furthermore, for lower squeezing parameters ( $r$ ) the difference between the fidelity of the photon subtracted TMSV and TMSC is large which closes down for higher squeezing. The Gaussian state outperforms both the non-Gaussian PSTMSV and PSTMSC states. The PSTMSC outperforms PSTMSV as seen in the figure, for  $d = 10$ . Results of several papers can be reproduced as special cases of our general result. We can obtain the fidelity expression for ideal photon subtraction on one mode of TMSV state by taking the limit  $\tau \rightarrow 1$  and  $d \rightarrow 0$  [22, 23].

$$F = \frac{1}{4(1 + \alpha^2 - \alpha\sqrt{1 + \alpha^2})^2} \quad (3.1)$$

where  $\alpha = \sinh r$

### 3.1.2 Photon Addition on one mode of TMSC state

In this case, we take  $m = 1$  and  $n = 0$  in the Fig. 2.1. One photon is added to the two mode squeezed coherent state at the output. The output state is called one-photon added two mode squeezed coherent (1-PATMSC) state. The characteristic function can be found by putting the appropriate values of  $m$  and  $n$  in the Eq. (2.6). Further we use Eq. (1.36) and (1.37) to get the fidelity of teleportation. The expressions for the fidelity are too complicated and long to be included in this document therefore we directly provide the plots of the Fidelity ( $F$ ) with respect to squeezing parameter ( $r$ ). Higher  $r$  represents higher entanglement between the two modes of the squeezed state. Since, the resource state represents a family of states which is characterised

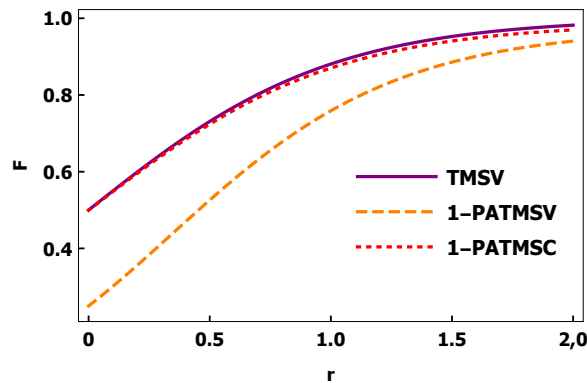


Figure 3.3: Fidelity ( $F$ ) vs squeezing parameter ( $r$ ) of teleportation for one-photon-added two mode squeezed coherent (1-PATMSC) state.

by  $d$ , we can also plot Fidelity ( $F$ ) for different displacements ( $d$ ) which shows a

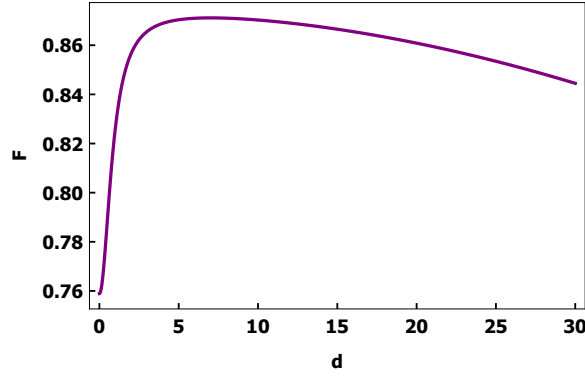


Figure 3.4: Fidelity ( $F$ ) vs displacement ( $d$ ) of teleportation for one-photon-added two mode squeezed coherent (1-PATMSC) state.

trend for different state functions in phase space. As seen in the trends above, the fidelity increases initially as we move away from the origin of phase space, then for higher displacements it starts decreasing. The graph is drawn for the fixed squeezing parameter  $r = 1$ . Furthermore, for lower squeezing parameters ( $r$ ) the difference between the fidelity of the photon added TMSV and TMSC is large which closes down for higher squeezing. The Gaussian state TMSV outperforms both the non-Gaussian PATMSV and PATMSC states. The PATMSC outperforms PATMSV as seen in the figure, for  $d = 10$ . Results of several papers can be reproduced as special cases of our general result. We can obtain the fidelity expression for ideal photon addition on one mode of TMSV state by taking the limit  $\tau \rightarrow 1$  and  $d \rightarrow 0$  [22, 23].

$$F = -\frac{1 + \alpha^2 - \alpha\sqrt{1 + \alpha^2}}{4(-1 - \alpha^2 + \alpha\sqrt{1 + \alpha^2})^3} \quad (3.2)$$

where  $\alpha = \sinh r$

### 3.1.3 Photon Catalysis on one mode of TMSC state

In this case, we take  $m = 1$  and  $n = 1$  in the Fig. 2.1. One photon is catalysed to the two mode squeezed coherent state at the output. The output state is called one-photon catalysed two mode squeezed coherent (1-PCTMSC) state. The characteristic function can be found by putting the appropriate values of  $m$  and  $n$  in the Eq. (2.6). Further we use Eq. (1.36) and (1.37) to get the fidelity of teleportation. The expressions for the fidelity are too complicated and long to be included in this document therefore we directly provide the plots of the Fidelity ( $F$ ) with respect to squeezing parameter ( $r$ ). Higher  $r$  represents higher entanglement between the two

modes of the squeezed state. Since, the resource state represents a family of states

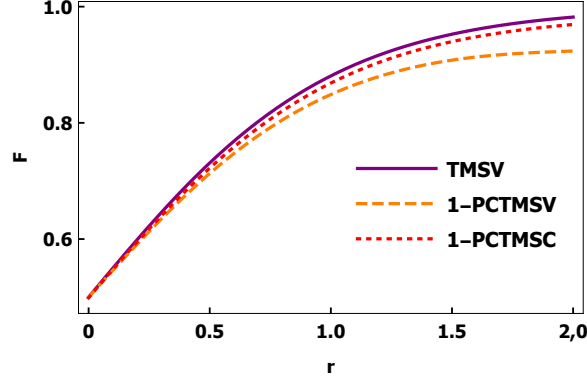


Figure 3.5: Fidelity ( $F$ ) vs squeezing parameter ( $r$ ) of teleportation for one-photon-catalysed two mode squeezed coherent (1-PCTMSC) state.

which is characterised by  $d$ , we can also plot Fidelity ( $F$ ) for different displacements ( $d$ ) which shows a trend for different state functions in phase space. As seen in the

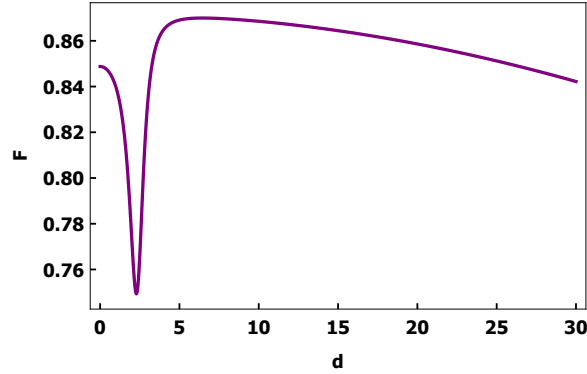


Figure 3.6: Fidelity ( $F$ ) vs displacement ( $d$ ) of teleportation for one-photon-catalysed two mode squeezed coherent (1-PCTMSC) state.

trends above, the fidelity decreases initially as we move away from the origin of phase space, there is a sharp dip around  $d$  between 2 and 3, it increases after the dip and finally for higher displacements it starts decreasing. The graph is drawn for the fixed squeezing parameter  $r = 1$ . Furthermore, for lower squeezing parameters ( $r$ ) the difference between the fidelity of the photon catalysed TMSV and TMSV is less which increases for higher squeezing. The Gaussian state TMSV outperforms both the non-Gaussian PCTMSV and PCTMSC states. The PCTMSC outperforms PCTMSV as seen in the plots, for  $d = 10$  [25, 8].

## 3.2 Symmetric Case

If the non-Gaussian operation is done on both of the modes of the TMSV and it is used as a resource for teleportation of a Gaussian state, we get the Symmetric case. The fidelity for different non-Gaussian operations is given as individual cases below.

### 3.2.1 Photon Subtraction on both modes of TMSV state

In this case, we take  $m_1 = m_2 = 0$  and  $n_1 = n_2 = 1$  in the Fig. 2.2. One photon is subtracted from each mode of the two mode squeezed coherent state at the output. The output state is called one-one-photon subtracted two mode squeezed coherent (1,1)-PSTMSC state. The characteristic function can be found by putting the ap-

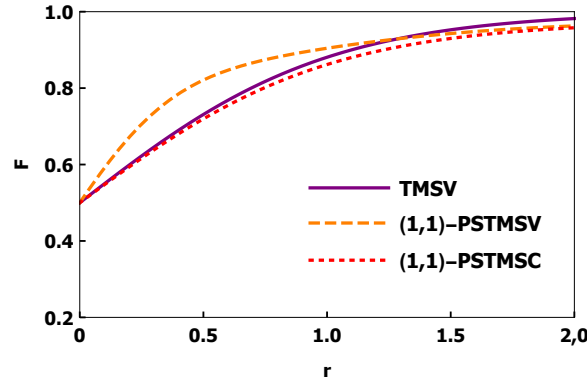


Figure 3.7: Fidelity ( $F$ ) vs squeezing parameter ( $r$ ) of teleportation for one-photon-subtracted (on both modes) two mode squeezed coherent (1,1)-PSTMSC state.

propriate values of  $m_1$ ,  $m_2$ ,  $n_1$  and  $n_2$  in the Eq. (2.12). Further we use Eq. (1.36) and (1.37) to get the fidelity of teleportation. The expressions for the fidelity are too complicated and long to be included in this document therefore we directly provide the plots of the Fidelity ( $F$ ) with respect to squeezing parameter ( $r$ ). Higher  $r$  represents higher entanglement between the two modes of the squeezed state.

Since, the resource state represents a family of states which is characterised by  $d$ , we can also plot Fidelity ( $F$ ) for different displacements ( $d$ ) which shows a trend for different state functions in phase space. As seen in the trends, the fidelity decreases as we move away from the origin of phase space. The graph is drawn for the fixed squeezing parameter  $r = 1$ . Furthermore, for lower squeezing parameters ( $r$ ) the photon subtracted TMSV outperforms both photon subtracted TMSC and the Gaussian TMSV state. The difference between the fidelity of the photon subtracted

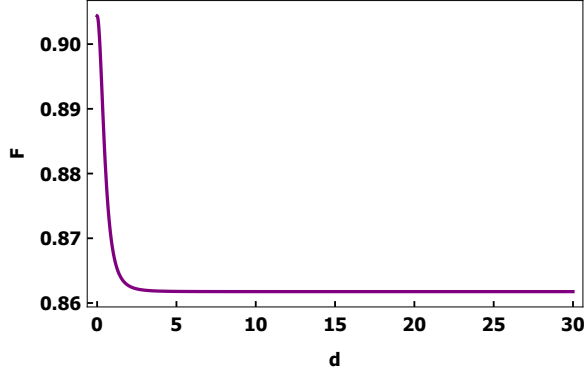


Figure 3.8: Fidelity ( $F$ ) vs displacement ( $d$ ) of teleportation for one-photon-subtracted (on both modes) two mode squeezed coherent (1,1)-PSTMSC state.

TMSV and TMSC is more initially which decreases for higher squeezing. The (1,1)-PSTMSV outperforms (1,1)-PSTMSC as seen in the figure, where  $d = 10$ . Results of several papers can be reproduced as special cases of our general result. We can obtain the fidelity expression for ideal photon subtraction on both modes of TMSV state by taking the limit  $\tau \rightarrow 1$  and  $d \rightarrow 0$  [22, 23].

$$F = \frac{(1 + \alpha^2 + \alpha\sqrt{1 + \alpha^2})(2 + \alpha(2\sqrt{1 + \alpha^2} + \alpha(3 + 2\alpha^2 + 2\alpha\sqrt{1 + \alpha^2})))}{4(1 + \alpha^2)^2(1 + 2\alpha^2)} \quad (3.3)$$

where  $\alpha = \sinh r$

### 3.2.2 Photon Addition on both modes of TMSC state

In this case, we take  $m_1 = m_2 = 1$  and  $n_1 = n_2 = 0$  in the Fig. 2.2. One photon is added to each mode of the two mode squeezed coherent state at the output. The output state is called one-one-photon added two mode squeezed coherent (1,1)-PATMSC state. The characteristic function can be found by putting the appropriate values of  $m_1$ ,  $m_2$ ,  $n_1$  and  $n_2$  in the Eq. (2.12). Further we use Eq. (1.36) and (1.37) to get the fidelity of teleportation. The expressions for the fidelity are too complicated and long to be included in this document therefore we directly provide the plots of the Fidelity ( $F$ ) with respect to squeezing parameter ( $r$ ). Higher  $r$  represents higher entanglement between the two modes of the squeezed state. Since, the resource state represents a family of states which is characterised by  $d$ , we can also plot Fidelity ( $F$ ) for different displacements ( $d$ ) which shows a trend for different state functions in phase space. As seen in the trends, the fidelity increases as we move away from the origin of phase space. The graph is drawn for the fixed squeezing parameter  $r = 1$ .

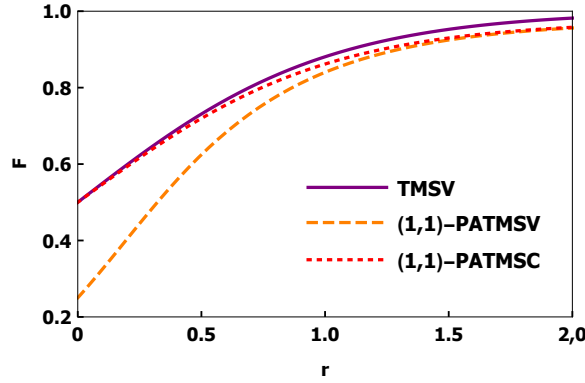


Figure 3.9: Fidelity ( $F$ ) vs squeezing parameter ( $r$ ) of teleportation for one-photon-added (on both modes) two mode squeezed coherent (1,1)-PATMSC state.

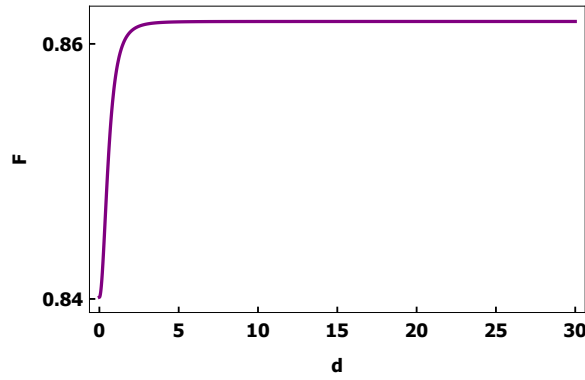


Figure 3.10: Fidelity ( $F$ ) vs displacement ( $d$ ) of teleportation for one-photon-added (on both modes) two mode squeezed coherent (1,1)-PATMSC state.

Furthermore, for lower squeezing parameters ( $r$ ) the photon added TMSV outperforms both photon added TMSV, both of which are outperformed by the Gaussian TMSV state. The difference between the fidelity of the photon added TMSV and TMSV is more initially which decreases for higher squeezing. The (1,1)-PATMSC outperforms (1,1)-PATMSV as seen in the figure, where  $d = 10$ . Results of several papers can be reproduced as special cases of our general result. We can obtain the fidelity expression for ideal photon addition on both mode of TMSV state by taking the limit  $\tau \rightarrow 1$  and  $d \rightarrow 0$  [22, 23].

$$F = -\frac{1 + \alpha^2}{4(1 + 2\alpha^2)(-1 - \alpha^2 + \alpha\sqrt{1 + \alpha^2})^3} \quad (3.4)$$

where  $\alpha = \sinh r$



### 3.2.3 Photon Catalysis on both modes of TMSV state

In this case, we take  $m_1 = m_2 = 1$  and  $n_1 = n_2 = 1$  in the Fig. 2.2. One photon is catalysed to each mode of the two mode squeezed coherent state at the output. The output state is called one-one-photon catalysed two mode squeezed coherent (1,1)-PCTMSC state. The characteristic function can be found by putting the appropriate values of  $m_1, m_2, n_1$  and  $n_2$  in the Eq. (2.12). Further we use Eq. (1.36) and (1.37) to get the fidelity of teleportation. The expressions for the fidelity are too complicated and long to be included in this document therefore we directly provide the plots of the Fidelity ( $F$ ) with respect to squeezing parameter ( $r$ ). Higher  $r$  represents higher entanglement between the two modes of the squeezed state. Since, the resource state

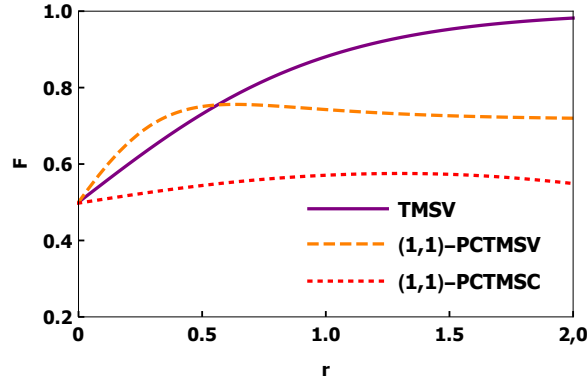


Figure 3.11: Fidelity ( $F$ ) vs squeezing parameter ( $r$ ) of teleportation for one-photon-catalysed (on both modes) two mode squeezed coherent (1,1)-PCTMSC state.

represents a family of states which is characterised by  $d$ , we can also plot Fidelity ( $F$ ) for different displacements ( $d$ ) which shows a trend for different state functions in phase space. As seen in the trends, the fidelity decreases initially as we move away from the origin of phase space and then increases to a constant value. The graph is drawn for the fixed squeezing parameter  $r = 1$ . Furthermore, for lower squeezing parameters ( $r$ ) the photon catalysed TMSV outperforms both photon catalysed TMSV and the Gaussian TMSV state. The difference between the fidelity of the photon subtracted TMSV and TMSV is more initially which dips a little and then maintains a difference for higher squeezing. The (1,1)-PCTMSV outperforms (1,1)-PCTMSC as seen in the figure, where  $d = 10$  [9, 8].

To summarise the results, for a non-Gaussian operation on one of the modes of the TMSV state, we get a teleportation fidelity which is better than its two mode squeezed

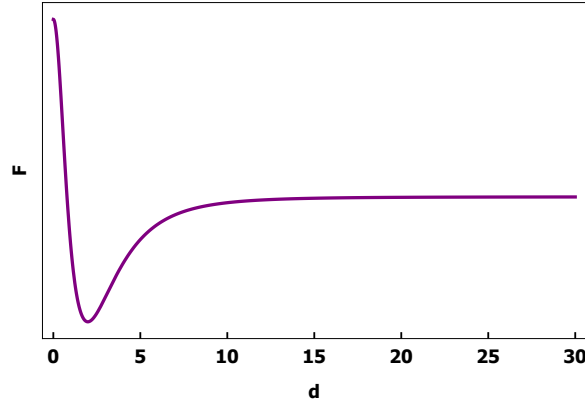


Figure 3.12: Fidelity ( $F$ ) vs displacement ( $d$ ) of teleportation for one-photon-catalysed (on both modes) two mode squeezed coherent (1,1)-PCTMSC state.

vacuum (TMSV) counterpart. A similar situation occurs for the two mode photon addition on the TMSV state. However, for both the above cases, the Gaussian TMSV state gives the best fidelity overall. For a symmetric photon subtraction and catalysis on the TMSV state, teleportation fidelity exceeds that of the Gaussian TMSV state and the non-Gaussian TMSV state. The role of coherence in teleportation study has not been explored before. The better yield of generation for the squeezed coherent states makes our investigation particularly important.

# Chapter 4

## Conclusion

In this thesis, we explored the role of coherence in the quantum teleportation of a coherent state. To this end, we explicitly derived the Wigner characteristic function of the non-Gaussian two mode squeezed coherent (NG-TMSC) state, which to the best of our knowledge does not exist in the literature. The non-Gaussian operations utilised in this thesis are photon subtraction, photon addition and photon catalysis on one and both the modes of a TMSC state. This general class of non-Gaussian operations, result in a NG-TMSC state. We use this as a resource state for the teleportation of a coherent state. The special case of NG-TMSV state can be derived by putting displacement  $d = 0$ . When non-Gaussian operations are performed on one mode of TMSC state, coherence indeed provides an advantage. In the case of non-Gaussian operations on both modes of TMSC state, the results are mixed. We get a situation similar to the asymmetric case for the symmetric photon addition. However, for symmetric photon subtraction and catalysis, NG-TMSV yields better fidelity than both the TMSV state and the NG-TMSC state for lower squeezing parameter.

Since the TMSC states can be generated by feeding coherent states, which are readily available from well phase-stabilised lasers, in the down-converter, they are easier to prepare than TMSV states, where one needs to deal with vacuum states.

In this thesis, we have considered ideal photon detectors for the generation of non-Gaussian states. It is of paramount importance to find the effect of non-unit efficiency detectors [16, 15] on the teleportation fidelity. The POVM of the photon number detectors (PNRD) can be taken such that the efficiency is considered in the expression itself. Furthermore, we could analyse the effect of environment by considering decoherence of quantum states. We also plan to analyse the necessary and sufficient criteria for non-Gaussian quantum teleportation by analysing several

quantum resources such as non-classicality, non-Gaussianity, EPR correlations, and HZ correlations.

# Bibliography

- [1] A. Arvind, K. Dorai, S. Chaturvedi, and N. Mukunda. The development of quantum mechanics: A story of people, places and philosophies. *Resonance*, 23:1077–1100, 10 2018. [2](#)
- [2] S. L. Braunstein and H. J. Kimble. Teleportation of continuous quantum variables. *Phys. Rev. Lett.*, 80:869–872, Jan 1998. [13](#)
- [3] S. L. Braunstein and P. van Loock. Quantum information with continuous variables. *Rev. Mod. Phys.*, 77:513–577, Jun 2005. [3](#)
- [4] S. Chaturvedi, E. Ercolessi, G. Marmo, G. Morandi, N. Mukunda, and R. Simon. Wigner-weyl correspondence in quantum mechanics for continuous and discrete systems - a dirac-inspired view. *Journal of Physics A: Mathematical and General*, 39:1405, 01 2006. [9](#)
- [5] S. Chaturvedi, E. Ercolessi, G. Marmo, G. Morandi, N. Mukunda, and R. Simon. Wigner–weyl correspondence in quantum mechanics for continuous and discrete systems—a dirac-inspired view. *Journal of Physics A: Mathematical and General*, 39(6):1405–1423, jan 2006. [11](#)
- [6] R. F. Fox. Generalized coherent states. *Phys. Rev. A*, 59:3241–3255, May 1999. [8](#)
- [7] C. Gerry and P. Knight. *Introductory Quantum Optics*. Cambridge University Press, 2004. [4](#)
- [8] L. Hu, Z. Liao, and M. S. Zubairy. Continuous-variable entanglement via multi-photon catalysis. *Phys. Rev. A*, 95:012310, Jan 2017. [29](#), [33](#)

- [9] L.-Y. Hu, J.-N. Wu, Z. Liao, and M. S. Zubairy. Multiphoton catalysis with coherent state input: nonclassicality and decoherence. *Journal of Physics B: Atomic, Molecular and Optical Physics*, 49(17):175504, aug 2016. [33](#)
- [10] H. Leinfelder. A geometric proof of the spectral theorem for unbounded self-adjoint operators. *Mathematische Annalen*, 242(1):85–96, Feb 1979. [9](#)
- [11] K. S. Mallesh, S. Chaturvedi, V. Balakrishnan, R. Simon, and N. Mukunda. Symmetries and conservation laws in classical and quantum mechanics. *Resonance*, 16(2):129–151, Feb 2011. [2](#)
- [12] K. S. Mallesh, S. Chaturvedi, R. Simon, and N. Mukunda. States of physical systems in classical and quantum mechanics. *Resonance*, 17(1):53–75, Jan 2012. [1](#), [2](#)
- [13] P. Marian and T. Marian. Continuous-variable teleportation in the characteristic-function description. *Physical Review A*, 74, 07 2006. [15](#)
- [14] M. A. Nielsen and I. L. Chuang. *Quantum Computation and Quantum Information: 10th Anniversary Edition*. Cambridge University Press, USA, 10th edition, 2011. [2](#)
- [15] S. Olivares and M. G. A. Paris. Enhancement of nonlocality in phase space. *Phys. Rev. A*, 70:032112, Sep 2004. [35](#)
- [16] S. Olivares, M. G. A. Paris, and R. Bonifacio. Teleportation improvement by inconclusive photon subtraction. *Phys. Rev. A*, 67:032314, Mar 2003. [35](#)
- [17] S. Pirandola and S. Mancini. Quantum teleportation with continuous variables: A survey. *Laser Physics*, 16(10):1418–1438, Oct 2006. [15](#)
- [18] T. C. Ralph. Quantum optical systems for the implementation of quantum information processing. *Reports on Progress in Physics*, 69(4):853–898, mar 2006. [3](#)
- [19] J. E. Roberts. Rigged hilbert spaces in quantum mechanics. *Communications in Mathematical Physics*, 3(2):98–119, Apr 1966. [9](#)
- [20] J. J. Sakurai and J. Napolitano. *Modern Quantum Mechanics*. Cambridge University Press, 2 edition, 2017. [2](#), [8](#), [9](#)

- [21] A. Serafini. *Quantum Continuous Variables: A Primer of Theoretical Methods*. 07 2017. [14](#), [15](#), [17](#)
- [22] S. Wang, L.-L. Hou, X.-F. Chen, and X.-F. Xu. Continuous-variable quantum teleportation with non-gaussian entangled states generated via multiple-photon subtraction and addition. *Phys. Rev. A*, 91:063832, Jun 2015. [27](#), [28](#), [31](#), [32](#)
- [23] S. Wang, H. yi Fan, and L. yun Hu. Photon-number distributions of non-gaussian states generated by photon subtraction and addition. *J. Opt. Soc. Am. B*, 29(5):1020–1028, May 2012. [27](#), [28](#), [31](#), [32](#)
- [24] C. Weedbrook, S. Pirandola, R. García-Patrón, N. J. Cerf, T. C. Ralph, J. H. Shapiro, and S. Lloyd. Gaussian quantum information. *Rev. Mod. Phys.*, 84:621–669, May 2012. [12](#)
- [25] X.-x. Xu. Enhancing quantum entanglement and quantum teleportation for two-mode squeezed vacuum state by local quantum-optical catalysis. *Phys. Rev. A*, 92:012318, Jul 2015. [29](#)